Characterisation of the uranium tetrafluoride unburnt materials using non-destructive assay techniques for safeguards purposes.

MM Tshabalala

orcid.org 0000-0002-1474-2764

Mini-dissertation accepted in partial fulfilment of the requirements for the degree *Master of Science in Applied Radiation Science and Technology* at the North-West University

Supervisor: Prof MV Tshivhase

Co-supervisor: Mr PP Magampa

Graduation ceremony: July 2020

Student number: 23772956

DECLARATION

I, Makgobe Matshediso Tshabalala, declare that this dissertation "**Characterisation of uranium tetrafluoride unburnt materials using non–destructive assay techniques for nuclear safeguards purposes"** is my own work and has not been previously submitted for a Masters' degree at any tertiary institution in South Africa and the world at large. All the authors of the material used in this work were fully acknowledged.

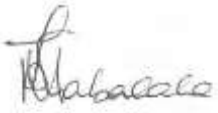

Signature Date: 31 October 2019

ACKNOWLEDGEMENTS

Firstly, I would like to thank God for the opportunity He granted me to pursue and finish this degree. The strength and resilience He continuously instilled in me, is what got me through to the finish line. I would like to thank my family, especially my parents, for the support they have given me throughout this journey. Each time it got tough on me, they were always there to encourage and remind me of the end goal.

I would like to thank the North-West University for allowing me to study at its premises. You have moulded and shaped me into the person I am today, both academically and personally. The teachings and advises I got during my study in your institution will forever be engraved in my heart.

To my supervisors, Prof V.M Tshivhase and Dr P. Magampa; and Dr TC Dlamini, I would not have done this if it were not for your guidance and constant support. Even when all seemed to not be going according to plan, you helped in keeping me calm and teaching me that research requires one to be patient and focused. Prof. Tshivhase once said, “if it’s too easy and smooth, you will not learn the beauty of patience”. I now know the beauty of patience. Dr Dlamini, your guidance played a major role in the completion of this work. Thank you.

To National Research Fund, your financial assistance has made it possible for me to pursue and complete my degree without worry. Not all this would have happened without the scholarship you awarded me. Thank you. To Nuclear Energy Corporation of South Africa, thank you for allowing me to conduct my research at your facilities. Ms Busisiwe Masemola, thank you for teaching me all I now know regarding my project and helping me with data collection. You have contributed immensely on this journey.

To all my friends and colleagues at Necsa, thank you for continuously encouraging me and making this sail worthwhile.

ABSTRACT

Inspectors use non-destructive assaying (NDA) techniques for verification measurements of safeguarded nuclear materials. The NDA techniques help the International Atomic Energy Agency to verify all declared nuclear materials and undeclared nuclear materials and activities. In Situ Object Counting System (ISOCS) and Multi-Group Analysis for Uranium (MGAU) as NDA instruments, play a pivotal role in safeguarding special nuclear materials. In this work, NDA techniques, in particular ISOCS and MGAU, were used to characterize and quantify the uranium tetrafluoride (UF_4) unburnts. The natural uranium, in uranium tetrafluoride (UF_4) (unburnts form), produced from the South African former conversion plant is the investigated material. The UF_4 (unburnts) were produced from ammonium diurinate (ADU) through calcination, reduction and hydrofluorination reactions. Therefore, the unburnts are as a result of the UF_4 that did not burn during the fluorination process to form uranium hexafluoride and are regarded as early nuclear fuel–cycle waste.

Uranium products before the enrichments stage in the nuclear fuel cycle were not subjected to nuclear safeguards implementation. According to the International Atomic Energy Agency (IAEA) Policy Paper 18 of 2009, the starting point of implementation of nuclear safeguards was redefined from the enrichment step to conversion step in the nuclear fuel cycle. The purpose of this study was to characterise the UF_4 (unburnts) from the conversion step in terms of the ^{235}U, ^{238}U and ^{232}Th isotopic mass content and enrichment of ^{235}U using ISOCS and MGAU. A set of 15 waste drums of the UF_4 unburnts were assayed using the broad energy germanium (BeGe) detector, the ISOCS and MGAU softwares. The isotopic mass content of ^{235}U, ^{238}U and ^{232}Th plus ^{235}U enrichment were measured by ISOCS while MGAU measured only ^{235}U enrichment.

The samples' fill heights through the use of peak 356 keV from the ^{133}Ba source were measured effectively for all the 15 UF_4 (unburnts) drums and ranged between 52.80 cm to 85.00 cm for 200 litre metal drums. UF_4 (unburnts) fill heights enabled the density of individual drums to be calculated and it ranged between 1.22 g/cm^3 to 3,41 g/cm^3 and the density measurements depend on the drums' net weight.

The 15 drums analysed by ISOCS had isotopic mass of ^{235}U ranging between 0.007±0.003 kg to 0.024±0.003 kg while ^{238}U mass ranged between 0.742±0.044 to

1.900±0.105 kg with one drum not detected. The enrichment values measured by ISOCS ranged between 0.436±0.044 and 1.358±0.027 weight percentage (wt.%).

For MGAU v4.2 results, ^{235}U enrichment fluctuated between 0.00 and 1.438±0.115 wt.%; and 0,000 to 1.635±0.121 wt.% for MGAU v4.3 results. ISOCS and MGAU software measured successfully the masses and the enrichment level of some uranium isotopes in UF_4 (unburnts). The uncertainties reported were within the accepted sigma of one.

Keywords*: Nuclear Safeguards; Non-destructive Assay Techniques, Uranium Tetrafluoride; Ammonium Diurinate; Conversion.*

TABLE OF CONTENTS

LIST OF TABLES

LIST OF FIGURES

LIST OF ABBREVIATIONS

ADU	Ammonium Diuranate
AEC	Atomic Energy Corporation
BEGe	Broad Energy Germanium
DA	Destructive Analysis
DoE	Department of Energy
HPGe	High-Purity Germanium detector
IAEA	International Atomic Energy Agency
ILW	Intermediate Level Waste
ISOCS	*In-Situ* Object Counting System
LLW	Low Level Waste
MGAU	Multi Group Analysis of Uranium
NECSA	South African Nuclear Energy Corporation
NDA	Non-Destructive Assaying
NFC	Nuclear Fuel Cycle
NPT	Non-Proliferation Treaty
NU	Natural Uranium
NUCP	Natural Uranium Conversion Plant
PP18	Policy Paper 18
SAFARI-1	South African Fundamental Atomic Research Installation – 1
UOC	Uranium Oxide Concentrates
UNH	Uranyl Nitrate

CHAPTER 1: INTRODUCTION AND PROBLEM STATEMENT

1.1 Background

The nuclear energy sector in South Africa (SA) has grown since its inception in the-1940s. With the discovery of accurate forecasts on the uranium potential in SA, the South African Atomic Energy Board (AEB) was formed to exercise control over the production and trade of uranium under an Act 43 of Parliament, 1948 (Bharath-Ram et al., 1997). The AEB handled the production and trade of uranium until the Act was amended in 1959 to make provision for research, development and utilisation of nuclear technology (National Nuclear Regulator, 2019).

The first nuclear research reactor of SA was built in cooperation with the Atoms of Peace programme under the Department of Energy of the United States of America. This reactor is called the South African Fundamental Atomic Research Installation – 1 (SAFARI–1) and it came into full operation on 18 March 1965 (Necsa, 2018). This reactor is a 20–megawatt (MW) thermal, tank–in–pool type nuclear research reactor. The SAFARI–1 served as a pilot into the development of nuclear technology in SA. Years after the commissioning of the SAFARI–1, the construction of the second South African reactor with two units commenced at Koeberg Power Station, Cape Town in 1976. Both units were synchronised to the grid on 4 April 1984 and 25 July 1985 respectively (Eskom, 2018). The Koeberg power reactors have a capacity of 1940 MW combined. The reactors at Koeberg station are a type of pressurised water reactor (PWR) and belong to the generation two reactors. The Koeberg power plant is utilised for generating electricity.

The formation of Uranium Enrichment Corporation (UCor) in the 1970s saw a large programme of uranium conversion, enrichment and fuel fabrication initiated. SA started producing its own nuclear fuel from its mined uranium. The subsidiary companies of AEB, namely UCor and Nuclear Development Corporation were incorporated into AEB in 1985 and AEB was later named the Atomic Energy Corporation (Bharath-Ram et al., 1997). The principal goal of AEC was to develop an indigenous nuclear fuel cycle for powering nuclear power plants, providing material for former nuclear weapon activities and to perform research that supported the aforementioned activities (AEC, 1997).

Over two decades (1965–1985), the AEC had two enrichment plants in operation. One plant was producing low–enriched uranium for nuclear fuel production, while the other plant produced high–enriched uranium for weapons programme.

1.1.1 Non-Proliferation Treaty declaration

In 1989, the South African government voluntarily dismantled all its nuclear weapons facilities. This act of dismantling the nuclear weapons facilities saw the country signing the nuclear Non-Proliferation Treaty (NPT - referred as the Treaty) and accepting International Atomic Energy Agency (IAEA) safeguards application agreement in 1991 (IAEA, 1991). The IAEA officials conducted various inspections and in 1993, they declared South Africa a non-nuclear weapon state (von-Baeckmann et al., 1995).

According to the IAEA the state parties that form part of the Treaty agree to accept safeguards (IAEA, 1970). The agreement to accept safeguards is for the exclusive purpose of verification of the fulfilment of commitments assumed under the Treaty, with an understanding to prevent diversion of nuclear energy from peaceful uses to nuclear weapons or other nuclear explosive devices (IAEA, 1991; IAEA, 2015).

Nuclear safeguards were applied from enrichment step of the nuclear fuel cycle as products that were produced in this step were suitable to be used for explosives (Dewji, 2014). With the changing technology, conversion step was announced as the first point of nuclear safeguards (IAEA, 2009a). Safeguards implementation is not applicable to materials in mining or ore processing activities. The materials produced in the aforementioned activities have impurities and compositions that are not suitable for isotopic enrichment and fuel fabrication (IAEA, 1991).

In 1991, the Y (enrichment) plant was closed and decommissioning commenced. The closure of the enrichment plant was to cement the NPT agreement as enriched nuclear weapons' material was produced at this plant (AEC, 1992). In 1995, the SA government cabinet approved the decommissioning of the last enrichment (Z) plant while in 1997 the board of AEC phased out the conversion plant (AEC, 1998). During the times in which these plants were operating, a large amount of nuclear waste was generated and such had to be stored for safety.

Potential proliferation of nuclear weapon material produced as a by-product of the nuclear fuel cycle remains a major obstacle to the expansion of nuclear power due to concerns of the public. Although the non-proliferative nature of the nuclear fuel cycle's material flow is supported by combination of administrative controls and safeguards measures, production of any material of sufficient quality and quantity should be avoided to prevent possible military/terrorism use.

1.2 Statement of Problems

Necsa is in possession of approximately 350 drums of UF_4 material that did not burn up during UF_6 synthesis (unburnt UF_4), regarded as waste in drums enclosed in polystyrene over-packs (Nangu et al., 2014). These waste drums are result of the conversion plant that operated at Necsa prior to 1991. As part of the agreement with IAEA and Department of Energy (DoE), Necsa's nuclear safeguards department is entrusted with the responsibility of declaring the inventory of all safeguarded nuclear materials within the state and to ensure that these materials are not diverted from peaceful uses (IAEA, 1991).

SA is currently in possession of UF_4 material that was declared to IAEA on estimated values. True values of these materials should be declared to IAEA as they consist of ^{232}Th and ^{235}U isotopes. Therefore, safeguards measures are necessary to characterise and quantify these unburnt nuclear materials as well as furnishing the IAEA with new readings.

The unburnt UF_4 have thorium inherent from ADU feed stream and because of thorium's non-volatile nature it was concentrated in the UF_4 (unburnt). A destructive analysis (DA) of the unburnt UF4 was performed to give the estimation of the weight of uranium. The non-destructive assay (NDA) was further applied to measure isotopic weight and enrichment content of ^{232}Th, ^{235}U and ^{238}U in the unburnt UF4 material from which 140 drums was successfully done.

Therefore, this study is to further measure the remaining waste drums of UF_4 unburnt and declare them to IAEA on measured values.

1.3 Research aim and objectives

The aim of the study was to characterise the UF_4 unburnt in terms of gross mass, net mass, fill height, material density, uranium enrichment level, ^{232}Th mass, ^{235}U mass and ^{238}U mass.

The objectives of the study were to:

- Use the fill height measurements to calculate sample volume and densities
- Effectively use Broad Energy Germanium detector with *In-Situ* Object Counting System software for measuring the mass of ^{232}Th, ^{235}U and ^{238}U and enrichment of ^{235}U
- Explore the use of Multi Group Analysis of Uranium software version 4.2 and 4.3 on Broad Energy Germanium detector to estimate ^{235}U enrichment.

CHAPTER 2: THEORETICAL BACKGROUND

2.1 South Africa and the signing of the treaty

In 1968, the general assembly of United Nations adopted the Non-Proliferation Treaty (NPT), also referred to as the Treaty for prevention of wider dissemination of nuclear weapons and it entered into force on the 5th of March 1970 (UNODA, 2019). The treaty had 93 signatory states that ratified it, with 98 state parties later acceding the agreement. The formation of the Treaty was motivated by the belief that nuclear weapons proliferation would extremely increase the danger of nuclear war judging by rapid growth of nuclear arsenals between the 1950s and 1960s.

The Treaty binds both the Non-Nuclear Weapon State (NNWS) and Nuclear Weapon State (NWS). The NWS are explained as States, which have produced and exploded a nuclear weapon before 1st January 1967 (UNODA, 2019). Under the Treaty, the NNWS parties pledge to not produce or procure nuclear weapons or nuclear explosive devices whereas NWS parties pledge not to help, encourage or induce any NNWS party to produce or procure nuclear weapons or explosive devices (IAEA, 2019a).

The NPT has 11 articles to it, all stipulating the requirements from States parties. Article I thwarts NWS to not transfer or assist the NNWS to manufacture or procure nuclear weapons or explosive devices while Article II commits the NNWS from not receiving or accepting help from NWS to quest such weapons (ACA, 2019; UNODA, 2015). Article III tasked the International Atomic Energy Agency (IAEA) to verify that the pledges from Article I and II are adhered to by verifying through the inspections that the nuclear materials in NNWS' nuclear facilities are not diverted for weapons/explosive devices (ANODA, 2015; IAEA, 1991). Article III is carried out in accordance with the IAEA comprehensive safeguards agreement.

The States parties to the treaty, through Article IV are permitted to do research, development, use nuclear energy for non-weapons reasons and it gives support for possible exchange of information and technologies between States parties for nuclear-related purposes. Due to the restriction of the Comprehensive Test Ban Treaty mandate on all nuclear explosions, Article V has become successfully outdated (ACA ,2019).

Article V gives permission to NNWS to do research and development on the benefits of nuclear explosions conducted for peaceful purposes from NWS. Article VI binds States parties to discuss on effective measures relating to ending nuclear arms race at an early date and to nuclear disarmament in good faith while Article VII allows States Parties to have regional treaties (UNODA, 2015). Article VIII allows for Treaty parties to propose amendments to the Treaty and have them approved by majority votes of all States parties and Article X institutes withdrawal terms by States parties from the treaty (ACA, 2019). Article IX and XI deals with the administrative roles of signing the Treaty and official languages used respectively.

The NNWS are the ones mainly at the receiving end of the conditions of the Treaty. The aim of the Treaty was to discontinue and subsequently have nuclear weapons dismantled by all States. To current date, although the proliferation of nuclear weapons has decreased, the NWS are still in possession of its warheads with Iran, Pakistan, India, North Korea and Israel still have not acceded to the Treaty (Wielligh and Wielligh-Steyn, 2015). Under Article VI, the Treaty has still not capitalised fully on this condition, 49 years after its inception.

Between late 1970s and early 1980s, the nuclear weapons programme in SA was initiated and saw six warheads completed by 1988. This nuclear weapon programme was disbanded in 1989 and South Africa acceded the NPT on 10th July 1991 in Washington DC (UNODA, 2019). The reason behind the accession was to lift off sanctions that were passed onto the country. As a result, SA signed a comprehensive safeguards agreement with IAEA as per conditions of Article III of the Treaty.

2.2 Nuclear safeguards

2.2.1 Nuclear safeguards

Nuclear safeguards are a set of technical measures applied by IAEA on nuclear materials and facilities. The IAEA pursues to verify a State's legal obligation that nuclear materials and facilities are not altered and diverted from peaceful uses through these technical measures (IAEA, 2019b). These verification measures are handled by the IAEA independently. The safeguards agreements are accepted by the States to give IAEA

permission to inspect the nuclear material and facilities as stipulated in the agreement. Safeguards are implemented on an annual cycle and have four main processes as follows (IAEA, 2019b):

- collection and evaluation of safeguards-relevant information
- development of a safeguards approach for a State
- planning, conducting and evaluating safeguards activities and
- drawing of safeguards conclusion.

The safeguards conclusions done by the IAEA provide reliable assurance to the international community that States abide to their safeguards obligations. The verification and findings by the IAEA are carried independently.

SA entered into a bilateral agreement with United States of America (USA) in 1965, to accept IAEA safeguards transfer agreement (IAEA, 1965). This agreement was a co-operation between the states to develop and promote the peaceful uses of atomic energy. On this agreement, both States pledged not to use the material, equipment and facilities in their inventories to further any military purposes (IAEA, 1965; IAEA, 1967). Under this agreement, the IAEA sole responsibility was to apply the safeguards system as stipulated in the agreement. The agreement opened doors for the IAEA to safeguard the SAFARI-1 reactor and all activities pertaining to it.

In 1975, the political sanctions were imposed on SA by USA. SA could not export the fuel elements for the reactor. As a result, the bilateral agreement between SA and USA fell off, as the States could not transfer any material with one another. During this time, SA bettered its nuclear capability and started to produce 45% enriched uranium fuel for SAFARI-1 (Wielligh and Wielligh-Steyn, 2015). Although the safeguards transfer agreement was cancelled, SAFARI-1 was still under IAEA inspections to ensure that the reactor is used for peaceful purposes only.

After the successful enrichment of uranium, nuclear weapon capability was developed and subsequently in the late 1970s, the manufacturing of these weapons started. The IAEA failed to detect this diversion for close to two decades until the SA signed the NPT agreement and subsequently the comprehensive safeguards agreement in 1991.

Comprehensive safeguards are an important tool used by IAEA to support the upholding of the Treaty in NNWS. Nuclear safeguards are done in accordance with Information Circular 153 of 1972 and Article III of the Treaty, which were amended in the agreement of government of Republic of South and IAEA in 1991. Under the comprehensive safeguards agreement, SA pledged to use nuclear energy only for peaceful activities, to have all facilities, equipment and material to be safeguarded and to notify the IAEA of any transfer of nuclear related material.

2.2.2. Policy context

Nuclear safeguards application was not applicable to stages prior to enrichment process on the nuclear fuel cycle (Dewji, 2014). The UF_6, feedstock for subsequent enrichment at commercial plants and UO_2 were the only safeguarded materials from natural uranium conversion plants (NUCPs). IAEA made a change to this in 2003, when it enlisted feedstock (UOC) and intermediary products (UO_3, UF_4) as safeguards relevance (Dewji, 2014; Doo, et al., 2003). This was because of the constant changes made in the industrial practices where high-purity uranium bearing products were produced, as advances were done at the front end of the fuel cycle.

With new developments done on the technology and industrial practices to ensure that safeguards are operated with efficacy, IAEA safeguards ought to remain current with the new advances. According to the technical interpretation of the INFCIRC/153 paragraph 34(c), the implementation of safeguards at NUCPs by IAEA has been inconsistent (IAEA, 1972). The comprehensive safeguards under INFCIRC/153 had limited access of IAEA for early nuclear activities thus limiting IAEA's monitoring capacity (Dewji, 2014).

Paragraph 34 (c) of starting point of safeguards from INFCIRC/153 (corrected) states the following (IAEA, 1972):

(a) When any material containing uranium or thorium which has not reached the stage of the nuclear fuel cycle described in sub-paragraph (c) is directly or indirectly exported to a non-nuclear-weapon State, the State shall inform the Agency of its quantity, composition and destination, unless the material is exported for specifically non-nuclear purposes;

(b) When any material containing uranium or thorium which has not reached the stage of the nuclear fuel cycle described in sub-paragraph (c) is imported, the State shall inform the Agency of its quantity and composition, unless the material is imported for specifically non-nuclear purposes; and

(c) When any nuclear material of a composition and purity suitable for fuel fabrication or for being isotopically enriched leaves the plant or the process stage in which it has been produced, or when such nuclear material, or any other nuclear material produced at a later stage in the nuclear fuel cycle, is imported into the State, the nuclear material shall become subject to the other safeguards procedures specified in the Agreement.

During the 44th Annual Meeting of the Institute of Nuclear Materials Management, Doo et al., outlined the new approach to safeguarding NUCP intermediate compounds under the above stated clause (Doo et al., 2003). Only all purified aqueous uranium solutions or uranium oxides suitable for isotopic enrichment or fuel fabrication as products were considered by IAEA as candidates for safeguards (Dewji, 2014). This later created a loophole in the policy as high purity uranium products were produced at the early stages of conversion process.

From Doo et al., (2003) conference paper, they proposed that “full safeguards procedures should be applied no later than the first point in the conversion process at which such material leaves the process stage or the plant in which it is produced” and was later included in the IAEA policy paper 18 (PP18). As of 2003, the starting point of safeguarded nuclear material was reinterpreted and source material was given a new definition in this category (Dewji, 2014; IAEA, 2009a). The PP18 furthermore points to address to support advancing the starting point of safeguards (Dewji, 2014; Doo et al., 2003; IAEA, 2009a) include:

(1) a new definition of source material, which potentially brings yellowcake under safeguards;

(2) new requirements for design information verification (DIV) and provision; and

(3) use of a complementary access-type concept.

Therefore, the historic nuclear waste material from Necsa’s conversion plant automatically became the first point of nuclear safeguarded material.

2.2.3 Uranium tetrafluoride background

The AEC, currently known as Necsa, had a conversion plant that was capacitated for 1200 tU/a for uranium hexafluoride (UF_6) supply to uranium enrichment facility (Bredell, 1990). The uranium conversion process that was used at AEC can be summarised by equation (2.1) to (2.4) (Bredell, 1990):

$$(\mathbf{NH_4})_2\mathbf{U_2O_7}\ (\mathbf{ADU}) \rightarrow \mathbf{2UO_3} + \mathbf{2NH_3} + \mathbf{H_2O} \quad (2.\ 1)$$

$$\mathbf{3UO_3} + \mathbf{2NH_3} \rightarrow \mathbf{3UO_2} + \mathbf{3H_2O} + \mathbf{N_2} \quad (2.\ 2)$$

$$\mathbf{UO_2} + \mathbf{4HF} \rightarrow \mathbf{UF_4} + \mathbf{2H_2O} \quad (2.\ 3)$$

$$\mathbf{UF_4} + \mathbf{F_2} \rightarrow \mathbf{UF_6} \quad (2.\ 4)$$

Unfortunately, not all uranium tetrafluoride (UF_4) compound burned during the conversion process. The unburnt UF_4 therefore turned into radioactive waste. Predominately the waste consists of natural uranium (^{235}U and ^{238}U) isotopes and thorium (^{232}Th) isotope. ^{232}Th existence is due to some of the ammonium diuranate (ADU) that was fed into the production line of UF_6 (Nangu, et al., 2014).

UF_4 compound is a green crystalline solid and has minimum solubility in water. According to Sibbens et al (2015), UF_4 compound has melting point of 1309K, which is slightly higher when compared to other covalent and polymeric tetrafluorides (Morel and Chatain, 2012). UF_4 vapour pressure is significantly low and as a result makes it a challenge to turn it into a gas form for enrichment purposes. Uranium (IV) is not stable in aqueous solutions but when it reacts with elements such as fluorine (F_2) in anionic solids, it becomes a stable compound (Morel and Chatain, 2012).

Uranium oxide (UO_2) is used as fuel for pressurised heavy water reactors and UF_6 as enriched uranium fuel for light water reactors (IAEA, 2009b). UF_6 is more suitable than UF_4 for enrichment purposes due to its thermal stability and moderately high volatility (IAEA, 1999). UF_6 has three main advantages that allow it to be enriched (IAEA, 2009b):

- it is a gas at low temperatures (56.4° C is its sublimation temperature at normal pressure),
- fluorine has only one isotope, and
- fluorine has a low atomic weight

However, UF_6 has the ability to react with moisture to form uranyl fluoride (UO_2F_6) which is an extremely corrosive media (IAEA, 2009b). Therefore, the conditions in which this process occurs should be monitored strictly. UF_6 enrichment process facilitates fuel fabrication process that produces fuel assemblies used in nuclear power reactors.

Conversion of uranium is performed at France, Canada, USA, Russia and China and currently (Loden, 2011). During the tenure of South Africa's conversion plant operation, UF_4 unburnt were generated. Due to the fast deterioration of the market environment, the plant in SA was stopped in 1995. Researches to characterise and declare the unburnt for IAEA are currently underway and performed within Necsa.

2.3 The nuclear fuel cycle

The nuclear fuel cycle plays a pivotal role in the production of fuel elements for use in reactor. For NNWS, this cycle has seven steps are as follows: mining and milling, conversion, enrichment, fuel fabrication, power plant, spent fuel storage and final disposal. For NWS the cycle has eight steps and are as follows: mining and milling, conversion, enrichment, fuel fabrication, power plant, reprocessing and recycling, spent fuel storage and final disposal (IAEA, 2011)

2.3.1 Mining and milling of natural uranium ore

The nuclear fuel cycle starts with the mining of the uranium ore from the ground. The ore is extracted from the ground by either *in-situ* techniques or excavation. Excavation can be through open pit or underground mining. Open pit mining is opted when the ore is closer to the surface while underground mining is use for ore that is deep in the ground (WNA, 2017a). *In-situ* leaching process is using acid to dissolve the uranium ore underground and have the concentrates suspended above surface.

The mined uranium ore undergoes milling process, whereby the uranium ore is crushed, leached in acid and precipitated to produce the uranium oxide concentrate (U_3O_8) also known as yellow cake. The waste of the leached uranium ore forms part of mine tailings. The U_3O_8 is natural uranium compound in powder form. This U_3O_8 is the feedstock of the conversion process.

As stated in Article 33 of comprehensive safeguards agreement of 1991, safeguard measures do not apply to material in mining or ore processing activities (IAEA, 1991). The significant impurity levels in the precipitated uranium warrants no reason for diversion of the nuclear material.

2.3.2 Conversion of the yellow cake

Conversion process of natural uranium is essential in the nuclear fuel cycle. During this process, natural uranium is purified by removing all the impurities that NU has from the mining process. The conversion stage can be divided into two categories, conversion 1 and 2 (Erpenbeck, 2017). Front–end conversion centred on processing of material at natural isotopic composition level whereas back–end conversion involves reprocessing of material at the level of enriched isotopic composition.

2.3.1.1 Front–end conversion

The yellow cake (UOC) produced from the milling phase of the nuclear fuel cycle, acts as the precursor of the front–end conversion process at a natural uranium conversion plant (NUCP) (Dewji, 2014; Erpenbeck, 2017). Front–end conversion process takes place in two main pathways namely dry and wet conversion (IAEA, 2009a; Raffo-Caiado et al., 2009; Erpenbeck, 2017). The size of the conversion plant determines the path followed.

The main difference between dry and wet conversion process is how impurities from uranium oxide concentrates (UOC) are removed (Loden, 2011). Removal of impurities are done in the second stage of solvent extraction in the wet process and only pure intermediates products such as UO_3 and UO_2 proceeds with the process. Nitric acid solution is used to dissolve the UOC and once dissolved, UOC is treated through solvent extraction process with tributylphosphate (TBP) that was dissolved in kerosene as a solvent (Loden, 2011; IAEA, 2009b; Raffo-Caiado et al., 2009). The product yielded from the afore-mentioned process is a purified uranyl nitrate (UNH) (IAEA, 2009b).

The UNH is dissolved in ammonia to give off precipitated ammonium diurinate (ADU), which is a suitable compound to produce UO_3 pellets/powder through drying and

calcination processes (Bredell, 1990; Loden, 2011). The UO_3 is fed into a vertical moving bed reactor consisting of two sections, an upper reduction section where UO_3 is converted into UO_2 at $600^{O}C$ by means of preheated ammonia. The formed UO_2 passes through the nitrogen barrier component into the lower section of this bed reactor. The lower section is utilised for hydrofluorination of UO_2 with aqueous hydrofluoric acid under endothermic conditions to form UF_4 (Bredell, 1990; IAEA, 1999; IAEA, 2009b). Figure 2-1 summarises this process.

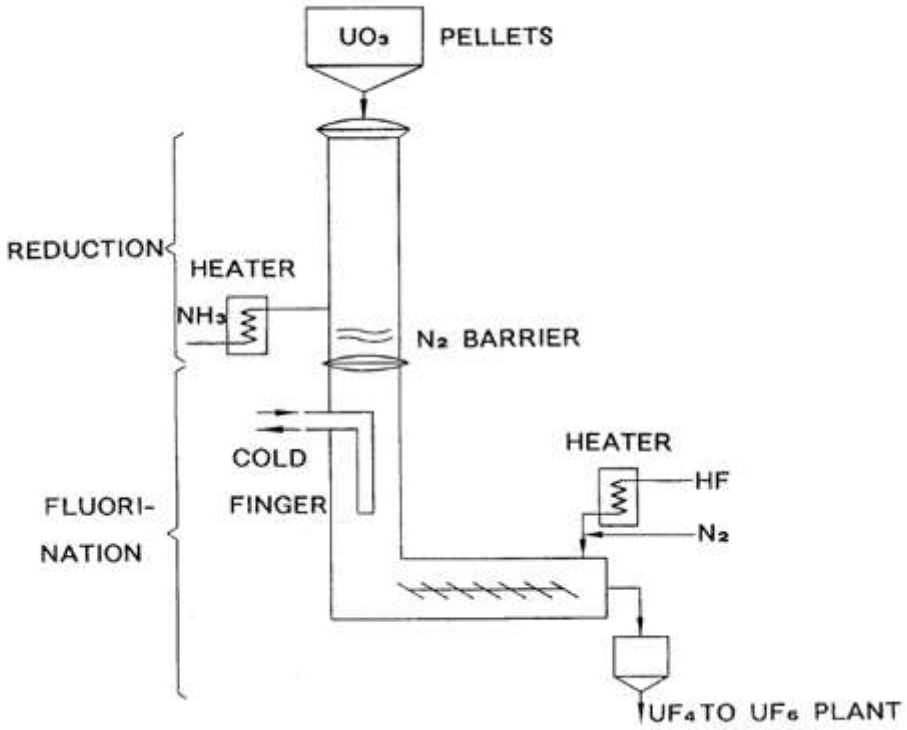

Figure 2-1: Schematic diagram of conversion of UO_3 to UF_4 reactor (Bredell, 1990).

The UF_4 compound produced is an intermediate product of UF_6 production. As mentioned, the intermediate product produced through chemical equations (2.1) to (2.3), UF_4 will further undergo a fluorination process, where by fluorine gas (F_2) manufactured electrolytically is fed into the UF_6 flame reactor. Bredell, 1990 and IAEA, 1999, described this endothermic reaction by equation (2.4). The UF_4 that is not converted to UF_6 is either recycled into the reactor or retained as unburnt UF_4 material (Bredell, 1990) and this process is illustrated in Figure 2-1 and 2-2, while Figure 2-3 sums up wet conversion process in full details.

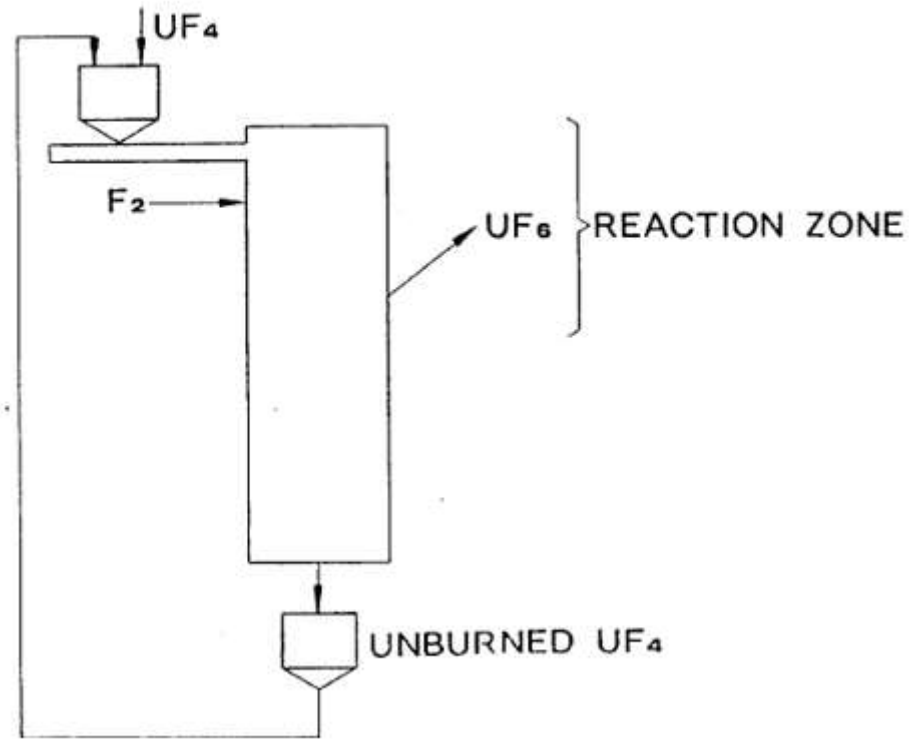

Figure 2-2: Schematic diagram of UF_6 conversion reactor (Bredell, 1990).

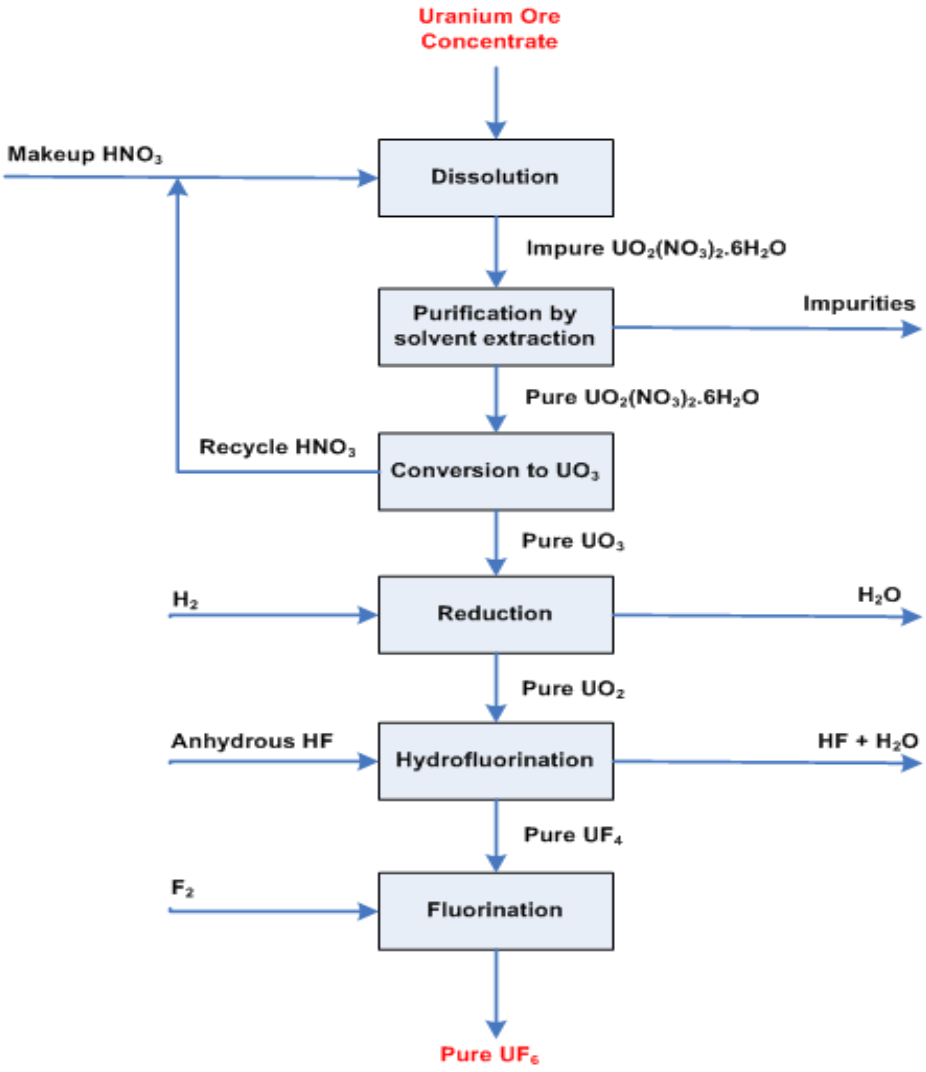

Figure 2-3: Wet conversion process diagram (IAEA, 2009b).

The dry conversion process is different from the wet conversion as impurities are removed after the production of UF_6 through distillation process (Loden, 2011). Unlike the wet process, the impure natural uranium in a form of U_3O_8 or UO_3 is reduced by heated nitrogen or hydrogen gas to form UO_2. The UO_2 is hydro–fluorinated to form UF_4 that subsequently reacts with fluorine gas through the fluorination reaction to form UF_6 (Loden, 2011). The UF_6 therefore, gets purified through the process of fractional distillation to give off UF_6 that is regarded as enrichment feed. This conversion process is currently utilised only by the Cameco plant in Canada and is described in Figure 2-4.

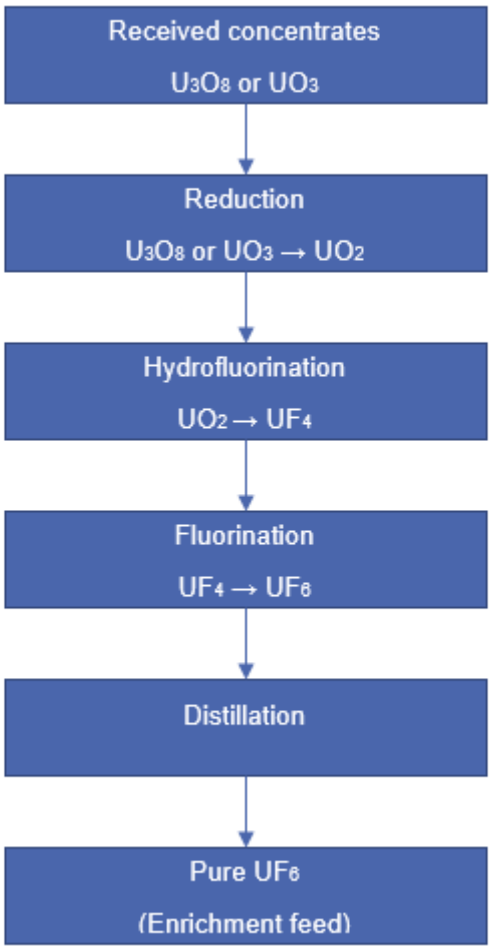

Figure 2-4: Dry conversion process diagram (IAEA, 1999).

The UF_4 unburnts are by virtue radioactive waste and as such, they are not easily disposed due to the hazards they impose to humans and environment. These unburnts do not produce high levels of radiation like enriched UF_6.

2.3.1.2 Back–end conversion

The back–end conversion process is mainly responsible for converting enriched UF_6 to UO_2 and converting reprocessed Pu and U to PuO_2 and UO_2 (Erpenbeck, 2017). Back–end conversion starts from reactants that are high level waste and enriched uranium and this process is often referred to as recycling and reprocessing.

The gaseous UF_6 that is produced from the reaction of UF_4 and F_2 goes through the enrichment process. This process ensures that an obtainable concentration and diluted fraction in ^{235}U through the centrifugal force reactor is attained (Orrego, et al., 2016). The ^{235}U is enriched from natural composition of 0.71% to between 2% and 5% depending on the type of reactor used (IAEA, 2009b).

The enriched UF_6 will then have to be converted to its UO_2 form to allow manufacturing of enriched uranium fuel. This is done through a series of chemical reactions, which include H_2 reduction and hydrolysing (Orrego et al., 2016; IAEA, 2009b). H_2 reduction process of UF_6 takes places only in two steps shown in equation (2.5) to (2.6):

$$\mathbf{UF_6 + H_2 \rightarrow UF_4 + 2HF} \quad (2.5)$$

$$\mathbf{UF_4 + 2H_2O \rightarrow UO_2 + 4HF} \quad (2.6)$$

Hydrolysing is subdivided into dry and wet re-conversion process. Water is used in both gas and liquid state to form UO_2. The dry re-conversion process is scientifically known as the integrated dry route (IDR) process and its UO_2 product is of high reactivity and fine particle size (IAEA, 2009b).

The wet re-conversion process is subdivided into two groups, namely the ADU and Ammonium Uranyl Carbonate (AUC) processes and are the most repeatedly used techniques to form UO_2 from UF_6. The UO_2 produced therefore undergo series of reactions to be enriched.

The ADU hydrolysing reaction can be summed in equations (2.7) to (2.8):

$$\mathbf{UF_6 + 2H_2O \rightarrow UO_2F_2 + 4HF} \quad (2.7)$$

$$\mathbf{2UO_2F_2 + 6NH_3 + 6H_2O \rightarrow (NH_4)_2U_2O_7 + 4NH_4F + 3H_2O} \quad (2.8)$$

The equation (2.8) will subsequently be reduced using H_2 at temperatures of 600–800°C and its reaction is represented by equation (2.9):

$$\mathbf{(NH_4)_2U_2O_7 + 2H_2 \rightarrow 2UO_2 + 2NH_3 + 3H_2O} \quad (2.9)$$

The AUC hydrolysing reaction can be summed up by equation (2.10) and (2.11):

$$\mathbf{UF_6 + 2H_2O \rightarrow UO_2F_2 + 4HF} \quad (2.10)$$

$$\mathbf{UO_2F_2 + H_2 \rightarrow UO_2 + 2HF} \quad (2.11)$$

Uranium in a form of UO_2 is easier to store and is often refer to as natural uranium form.

2.3.3 Enrichment of uranium hexafluoride

The resulting UF_6 in the conversion process acts as a feedstock for uranium enrichment process. The most preferred physical form of UF_6 is gas. The UF_6 has natural abundance of ^{238}U at 99,28% while 0,711% belongs to ^{235}U. The 0,711% of ^{235}U in this process is enriched to at least between 3-20% depending on the enrichment facility and the type of fuel produced according to Article 37 of comprehensive safeguards (IAEA, 1972). The rejected depleted uranium from this process ranges between 0,2-0,3%.

Different methods of enrichment were explored and gas centrifuge process is the most used method currently as it is more energy efficient (Loden, 2011; WNA, 2017b). The UF_6 gas is feed into a high speeding cylinder in partial vacuum. Due to the high speed of the cylinder, the ^{235}U molecules move near the center of the centrifuge while ^{238}U molecules move towards the outside. As the counter-current develops, the depleted stream is removed by scoops at the top while the enriched product is extracted by the scoop at the bottom. The extracted enriched product is converted into UO_2 powder and that acts as one of the feed for fuel fabrication.

2.3.4 Fuel fabrication of enriched uranium

Fuel fabrication process is solely for the production of fuel used in nuclear reactors. Starting uranium material are not limited to UO_2 but metallic uranium can be utilised (IAEA, 1999). The UO_2 powder from the enrichment facility is blended to form a powder batch that is homogeneous and later granulated. The granulated UO_2 is therefore, injected in the ceramic pellets, which are sintered at high temperatures in hydrogen atmosphere (WNA, 2017a). Once sintered, the pellets are enclosed in metal tubes to form fuel rods. The fuel assembly are the assembled fuel rods, ready for use in the reactor.

Metallic uranium in the form of UF_4 and magnesium (Mg) mixture are used as feedstock to produce uranium metallic rods. The Magnox reactor use this fuel for burn up. The UF_4/Mg mixture is blended and pelletized. These pellets undergo reduction process where MgF_2 comes off as by product of uranium metal pellets. Further Mg is released through cleaning and vacuum casting and production of uranium metallic rods follows.

The rod then inserted into cans, which are filled with helium gas and have welded end cap (IAEA, 1999). The cans are assembled to form the fuel assembly. The fuel assemblies are transported to nuclear reactor plants where they are inserted in the reactor core.

2.3.5 Spent nuclear fuel and storage

The removal of used fuel in the reactor is done at least between 18-36 months, as the amount of fission plutonium and other by-product nuclides start to increase. The spent fuel concentrates are divided typically between ^{235}U (1%), fission plutonium (0,6%), minor actinides and fission products (3%) and ^{238}U (>95%) and the reactor type determines the waste concentrates (WNA, 2017a).

The removed spent fuel emits heat and radiation, usually from fission products. The nature of the spent fuel makes it challenging to handle the waste immediately after removal from the reactor. This results in temporary storage of spent fuel in the reactor pool, to decrease the radiation and heat levels (IAEA, 2018). The held up of spent fuel in this pool varies between couple of months to several years. After cooling period, the fuel is either reprocessed or conditioned. Conditioning is done for additional storage or disposal of the waste (IAEA, 2009b).

2.4. Chemistry of radionuclides

2.4.1 Uranium

Uranium (U) is one of the naturally occurring radioactive materials and 0.711% naturally enriched in the Earth crust (Frimmel et al., 2014). ^{238}U accounts for 99.28% of uranium ore, followed by ^{235}U with 0.711% and ^{234}U with only trace levels (Raffo-Caiado et al., 2009). These isotopes decay via alpha route with ^{235}U decaying also by gamma emission (DOE, 2001). The half-life of ^{238}U is 4.47×10^9 years whereas that of ^{235}U 7.13×10^8 years (Mashaba, 2011). These isotopes' long half-lives make them an ongoing problem over concerns of radioactive disposal.

The element Uranium is silver, malleable and ductile. It resembles magnesium as is highly electropositive and taints quickly when exposed to air and its reactivity increases with temperature. Uranium has five oxidation states but only the +4 and +6 states are stable and are widely used. The uranium +4 oxidation state is observed mainly in reduction conditions and is also prone to precipitation. The crystallisation of the UF_4 unburnt is due to the reduction conditions of U_4^+.

^{238}U is not a fissile material therefore, its ability to not fission with thermal neutrons, makes it challenging to use in thermal reactors. In addition, ^{238}U is a fertile isotope and can produce plutonium-239 after neutron activation (Awan and Khan, 2015). On the contrary, ^{235}U is the only fissile material occurring in nature and it has binding energy that exceeds that of critical energy, making it fission with thermal neutrons easier (IAEA, 2009b). ^{235}U is the only isotope of uranium that is suitable for used as fuel in thermal reactors and is usually between (3–5%) enriched (IAEA, 2009b; Makhijani et al., 2004).

The U in UF_4 is 99.28% of ^{238}U emitting alpha and gamma particles. ^{238}U decays into progeny of three short–lived isotopes: ^{234}Th with half–life of 24.1 days, ^{234m}Pa with half–life of 1.2 minute and ^{234}Pa, which has 6.7 hours half–life decaying to ^{234}U with half–life of 2.45×10^5. ^{234}Th, ^{234m}Pa and ^{234}Pa are beta and weak gamma emitters. Due to the long half–life of ^{238}U, properties of ^{234m}Pa are used to study its parent nuclide. The ^{235}U isotope makes up 0.71% of U in the UF_4 and it decays into ^{231}Th by emitting an alpha and gamma.

According to IAEA, natural uranium enrichment should not exceed 0.5% in ten metric tons (IAEA, 1999). As a result, nuclear safeguards and the Treaty deals extensively in accounting and verifying that uranium material is not diverted for nuclear weapons/devices activities.

2.4.2 Thorium

Thorium (Th) is the member of the actinide group and is a naturally occurring radioactive material (IAEA, 2005). Thorium is broadly distributed with an average concentration of 10 parts per million (ppm) in the Earth's crust, in many phosphates, silicates, carbonates and oxide minerals. According to ANL thorium has three isotopes which occur naturally and

are ^{232}Th, ^{230}Th and ^{229}Th (ANL, 2001). ^{232}Th is the predominate isotope with half–life of 1.4×10^{10} years and it accounts for more than 99% of natural thorium content.

Table 2-1: Thorium isotopes (Hyde, 1960).

Isotope	Half-life	Method of production
^{223}Th	~0.1 sec	Daughter of ^{227}U
^{224}Th	~ 1 sec	Daughter of ^{228}U
^{225}Th	8 min	Daughter of ^{229}U
^{226}Th	30.9 min	Daughter of ^{230}U
^{227}Th	18.17 day	Natural radioactivity; daughter of ^{227}Ac
^{228}Th	1.9 year	Natural radioactivity; daughter of ^{228}Ac
^{229}Th	7340 year	Daughter of ^{233}U
^{230}Th	8.0×10^{4} year	Natural radioactivity; daughter of ^{234}U
^{231}Th	25.64 hour	Natural radioactivity; daughter of ^{235}U
^{232}Th	1.39×10^{10} year	Natural thorium is >99% ^{232}Th
^{233}Th	22.1 min	^{232}Th + neutrons
^{234}Th	24.1 day	Natural radioactivity; daughter of ^{238}U

^{232}Th is an unstable isotope and it decays by releasing radiation until a stable and non–radioactive lead–208 is formed. ^{232}Th decays into ^{228}Ra with 5.75 years half–life and ^{228}Ra into ^{228}Th with 1.913 years half–life through alpha and beta route respectively. ^{228}Th is an alpha and weak gamma emitter in the 84.2 keV energy region and present as background radiation (Shtangeeva, 2004). Thorium is an electropositive element and shows a common +4 oxidation state, it also exists in +3, +2 and +1 oxidation states. When exposed to air, thorium darkens due to oxidation. Thorium quantities are usually present in ADU feed into UF_6 production line (Nangu et al., 2014). As a result, the thorium quantities are concentrated in the UF_4 unburnt.

Like ^{238}U, ^{232}Th is a fertile material and has the potential of breeding synthetic fissile isotope ^{233}U in a thermal neutron reactor efficiently (IAEA, 2005). With ^{232}Th ability to breed ^{233}U through thermal neutron capture, which has the potential of being used in the manufacturing of devices/weapons of mass destruction and as such, it is imperative that safeguards ensure that it is not diverted from peaceful uses (IAEA, 1991). ^{233}U is categorised with plutonium-239 and high enriched uranium and 8kg of it was set as an

important quantity for safeguards as compared to 30kg of ^{235}U (IAEA, 1991; WNA, 2017c).

2.5 Radioactive decay and radioactivity

In 1896, Henri Becquerel discovered the phenomenon of radioactivity. Radioactivity is a process in which a nucleus of an unstable atom or a parent atom loses energy through emitting radiation into a stable daughter atom (Lawson, 1999). The unstableness of such atoms is due to the unequal number of protons and neutrons in its nucleus and as a result, the strong nuclear force holding the protons and neutrons together fails to uphold. The daughter atoms continue to decay until a stable state is achieved and this can be seen through several decay processes (Kamunda, 2017). In most reactions, the new formed stable nucleus may have an altered chemical form. The uranium, actinium and thorium series illustrates the process of formation of stable daughter atom from its parent atom.

Nuclides that emit radiation spontaneously are known to be radioactive. The radiation emitted is classified into two groups, namely ionising and non-ionising radiation. Ionising radiation is defined as high-energy radiation given by radioactive nuclides in search to reach a stable form. On the contrary non-ionising radiation is known to have only adequate energy to cause excitation but not enough to produce charged ions when interacting with matter (Ng, 2003). There are three types of decay associated with ionising radiation, namely; alpha, beta and gamma emission.

2.5.1 Alpha decay

Alpha particles are produced through the alpha decay process. These particles consist of two neutrons and two positively charged protons and are regarded as helium ($_2^4He^+$) nucleus. Alpha decay is a mode preferred for elements of high atomic number (Z>83) (Gilmore, 2008) and their examples include radium, thorium and uranium. Alpha particles have high energies that range between 4 and 10 MeV (Mashaba, 2011). The principal decay is represented by equation (2.12):

$$\mathbf{{}_{Z}^{A}X \rightarrow {}_{Z-2}^{A-4}Y + {}_{2}^{4}\alpha + Q} \qquad (2.12)$$

where: A – mass number; Z – atomic number; X – parent atom; Y – daughter atom; α – alpha particle; Q – fixed quantity of energy released.

The above equation can also be written in an elemental form as equation (2.13):

$$^{238}_{92}\mathrm{U} \rightarrow {}^{234}_{90}\mathrm{Th} + {}^{4}_{2}\mathrm{He} + \mathrm{Q} \qquad (2.\ 13)$$

Though alpha particles are heavy and they are released at very high speeds of almost 30 000 km/s from the atom. However, the speed of these particles can be reduced and be stopped by 30 mm of air or a sheet of paper or the top layer of the skin (Kamunda, 2017). Alpha particle source when ingested are dangerous. Damage to the biological tissue can also occur if these particles are emitted inside the body due to their ionising power.

2.5.2 Beta decay

Beta particles are electrons that are either negatively (negatrons) or positively (positrons) charged but with the same mass number. The beta particles decay takes place in a nucleus that has too many protons or neutrons. Beta decay is divided into beta positive and beta negative.

During beta positive decay, a proton decays into a neutron and a positron and a neutrino is also emitted to conserve momentum. Positrons are comparable to the anti -matter of the electron. Positrons are denoted by β^+ symbol and their mass is the same as the electron but it carries +1e charge (Kamunda, 2017). The emission of positrons is only probable if there is an adequately large energy difference of 1022 keV between the consecutive isobaric nuclides (Gilmore, 2008). This process can be written as shown in equation (2.14):

$$p^+ \rightarrow n + \beta^+ + v \qquad (2.\ 14)$$

However, beta negative decay is a contrast of beta positive decay process. Beta negative decay occurs in a nucleus that has more neutrons than protons. The neutron decays into a proton and a negatron and an antineutrino is also given off. This decay process is denoted by β^- symbol. Equation (2.15) represents this decay process:

$$n \rightarrow p^+ + \beta^- + {}^{0}_{0}v \qquad (2.\ 15)$$

The beta decay is not only limited to positrons and negatrons, electron capture can also result in this form of decay. Mostly, electron capture occurs when the required transformation energy is not sufficient for positron decay. This alternative route is available for nuclides that have fewer neutrons. Electron capture occurs when the electron of the K-shell is captured by the nucleus to convert it into a proton. This process happens in the K-shell as it is the closest to the nucleus. Other shells will require a decrease in the decay energy to be eligible for capture probability (Gilmore, 2008). The electron capture equation is represented by equation (2.16):

$$\boldsymbol{p}^{+} + \boldsymbol{e}^{-} \rightarrow \boldsymbol{n} + \boldsymbol{v} \qquad (2.16)$$

Unlike alpha particles, beta particles do not ionise easily and can cause damage when ingested. Due to their small size, they are more penetrating when compared to alpha particles and can travel 10 mm into the body. Thin layers of aluminium or plastic can stop beta particles.

2.5.3 Gamma emission

Gamma rays have no charge and mass and are regarded as real rays (Parachoff, 1997) and these rays are produced through gamma decay. The gamma rays are emitted as a by-product of both alpha and beta decays. Alpha and beta particles' surplus energy is lost in the excitation phase as they seek to be in stable state and as a result, they emit a gamma ray as a by-product (Gilmore, 2008). Due to their electromagnetic nature, they have short wavelengths that resemble X-rays but carry more energy instead.

Their energies range between 0.1 to 3 MeV in radioactive decay. Unlike alpha and beta particles, gamma rays are deeply penetrating. These rays cause more harm to a human body tissues when not shielded. Unlike alphas and betas, materials that have high density can only stop gamma rays and the choice of shielding materials are steel, lead and concrete, with lead being the most used.

2.5.4 Radioactive equilibrium

Radioactive equilibrium is a relationship of decay rate between a radioactive parent nuclide and all of its daughter nuclides to achieve a stable state in a decay chain series. This simply means that the daughter nuclides may be produced at the same rate of decay (Prince, 1979; Dlamini, 2014). Radioactive equilibrium is reached in two states within a decay chain namely transient radioactivity equilibrium and secular radioactivity equilibrium (Gilmore, 2008).

Transient radioactivity equilibrium state refers to when the half-life of the parent nuclide is longer than half-life of the daughter nuclide, the activity between these nuclides is in constant ratio while secular radioactive equilibrium exists when the parent nuclide has a great long half–life compared to its daughter nuclides. The secular radioactive equilibrium state is illustrated in the natural radioactive series of uranium, actinide and thorium. The decay constant of the parent nuclide is relatively lower when compared to its daughters therefore; this leads all the daughter nuclides to decay at the rate of their parent.

Figure 2-5 shows the secular equilibrium state between a parent nuclide and its daughter nuclide. The activity of daughter nuclide in a decay chain series is given by equation (2.17) (Lilley, 2013);

$$\boldsymbol{N_D(t) = N_P(t_0)\frac{\lambda_P}{\lambda_D-\lambda_P}(e^{-\lambda_P t} - e^{-\lambda_D t})}. \qquad (2.\ 17)$$

In secular equilibrium this equation can be simplified into equation (2.18) (Lapp and Andrews, 1972);

$$\boldsymbol{N_D(t) = N_P(t_0)\frac{\lambda_P}{\lambda_D}(1 - e^{-\lambda_D t})}, \qquad (2.\ 18)$$

with time the $e^{-\lambda_D t}$ term will become negligible and the number of daughter nuclei will decay at a constant rate (Cember and Johnson, 2009; Lapp and Andrews, 1972; Turner, 2007):

$$\boldsymbol{N_D(t) = N_P(t_0)\frac{\lambda_P}{\lambda_D}}. \qquad (2.\ 19)$$

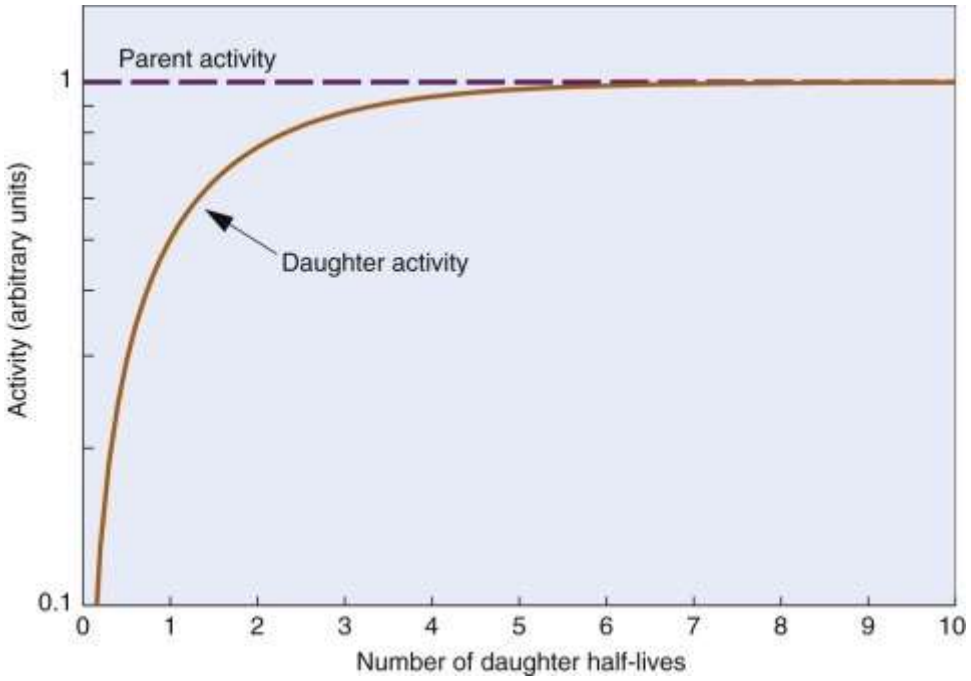

Figure 2-5: Secular equilibrium between a short-lived daughter and a long-lived parent nuclide (Cherry et al., 2012).

At a state of secular equilibrium, the daughter and parent have the same activities;

$$\boldsymbol{N_D\lambda_D = N_P\lambda_P}. \qquad (2.\ 20)$$

2.6 Radioactivity detection

2.6.1 Interaction of radiation with matter

Gamma rays and X-rays are electromagnetic in nature and not identified as different rays by the detector. These rays travel long distances and cannot be fully absorbed. Therefore, gamma rays interact with matter in three main mechanisms namely; photoelectric effect, Compton scattering and pair production.

2.6.1.1 Photoelectric effect

Photoelectric effect also known as photoelectric absorption is a phenomenon known to occur when a gamma–ray photon hits the electron of an atom and disappears and these

photons are dominant at energies lower than 100 keV (Gilmore, 2008). When the gamma–ray photon and a bound electron collide, an electron is ejected from the atom and the gamma ray loses all of its energy in the process and as a result an atom is ionised and excited energy state is reached. The excited atom redistributes its excitation energy to reach ground state by releasing further electrons (Auger cascade) to fill the unoccupied vacancy with a free electron from higher energy shell while emitting characteristic X–ray in the process (Ragheb, 2011). Figure 2-6 represents this phenomenon.

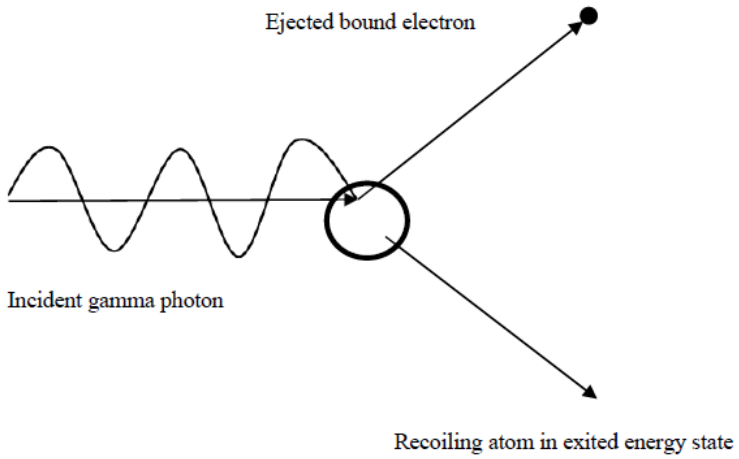

Figure 2-6: Schematic diagram of photoelectric effect (Ragheb, 2011).

In Auger cascade, the excitation energy is redistributed within the remaining electrons in the atom. An Auger electron fills the vacancy left in the shell. Further electrons released during this process, transfers further fraction of the total energy gamma–ray energy to the detector. In the emission of characteristic X–ray, the X–ray may undergo photoelectric effect while emitting additional X–rays, which are absorbed. This process will continue until all the gamma rays' energy has been absorbed. This interaction mostly occurs in the innermost shells like the K–shell, but if the energy needed to eject the K electrons is not enough, then electrons from either the L or M shell are ejected.

2.6.1.2 Compton scattering

Arthur H. Compton discovered Compton scattering while conducting research on the scattering of X–rays by light atoms in 1922 (Parks, 2004). Compton scattering is the main

form of interaction of gamma ray photons with matter. The scattering occurs between a gamma ray photon and an electron of the outer shell of the atom and results in the scattering of the gamma ray photon (Ragheb, 2011). The energy and momentum of the scattering is transferred to the electron while the photon continues with reduced energy, change in momentum and over an angle. Figure 2-7 illustrates the Compton scattering principle.

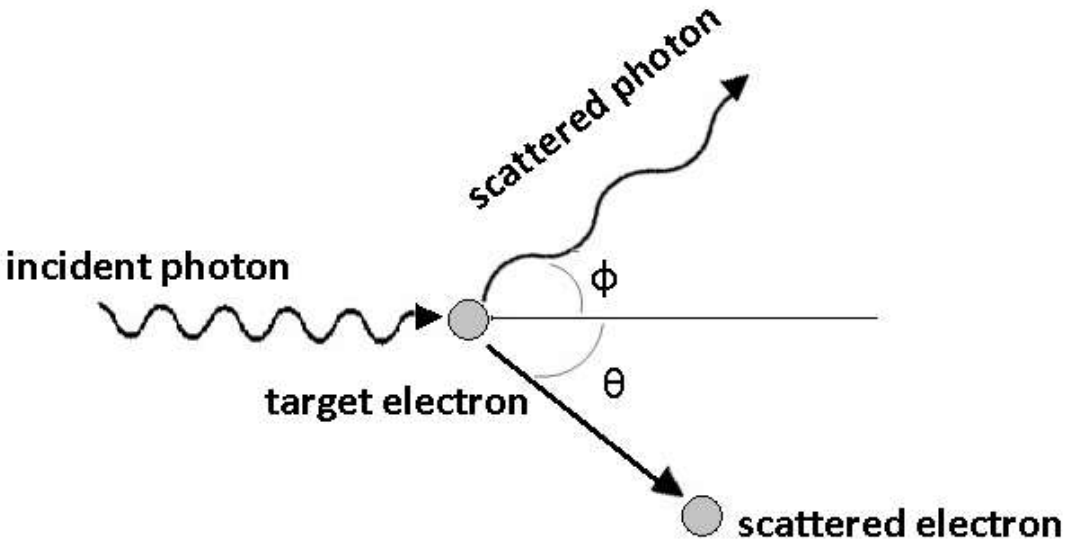

Figure 2-7: Schematic diagram of the Compton scattering process (Venugopal & Bhagdikar, 2013).

Compton scattering involves weakly bound electrons, the nucleus has only a negligible impact and the chances for interaction are almost independent of atomic number but depend greatly on the density of the material/electron (Gilmore, 2008; Nelson and Reilly, 1991). The probability of Compton scattering occurring increases, as the density of the material gets high. Due to Compton scattering mostly involving the outer and weakly bound electrons, its binding energy is insignificant when compared to the gamma–ray energy and this leads to the alteration of the shape of Compton response function. Unlike photoelectric effect and pair production, Compton scattering is a likely process to occur over a range of energies.

2.6.1.3 Pair production

Pair production is caused by gamma rays with energies beyond 1.02 MeV, also called high energy gamma rays with the aid of strong electromagnetic forces in the locality of a nucleus (Nelson and Reilly, 1991). The nucleus of the atom remains unaffected during this process. This interaction allows the formation of a positron and negatron through absorbing the gamma ray indefinitely. Both the positron and negatron travel precisely small distances before they lose their kinetic energy to the absorbing atom in a process called annihilation (Kamunda, 2017). The slowing down of the positron and negatron annihilate to form two protons regarded as annihilation photons that carries the charge of 511 keV respective (Onjefu, 2016) and Figure 2-8 explains this process.

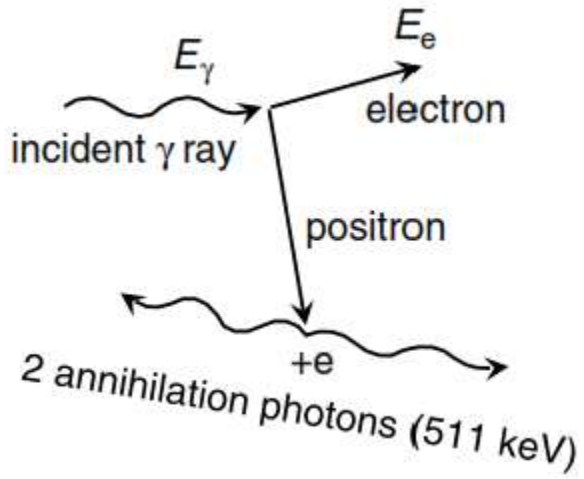

Figure 2-8: Schematic diagram of the pair production process.

Gamma photons have specific energies and intensities that are released from nuclear materials. Because nuclear materials occur in different radioisotopes, therefore, the intensity and energy released differs. The gamma ray spectrum calibrated by energy and intensity are used to categorize the gamma emitted isotopes by comparing the characteristic energies of nuclides (Tohamy et al., 2016). The pair production process takes place only under the control of the field of a nucleus but the energy threshold is twice larger than 2044 keV and its probability is much lower. Due to these reasons, the contribution of pair production is much smaller and thus not considered when analysing a gamma-ray spectrometry (Onjefu, 2016). In contrast, pair production is the most evident of all the interaction mechanism for energies larger than 10 MeV.

The initial gamma ray energy and the atomic number (Z) of the material plays a pivotal role in determining the strength of the probable form of gamma ray interaction. Photoelectric effect is predominating at low atomic number materials that have low gamma ray photon energy. Pair production is predominating in gamma ray photon energy exceeding 5 MeV while Compton scattering dominates in the middle range energies. Figure 2-9 shows the significant area of each interaction.

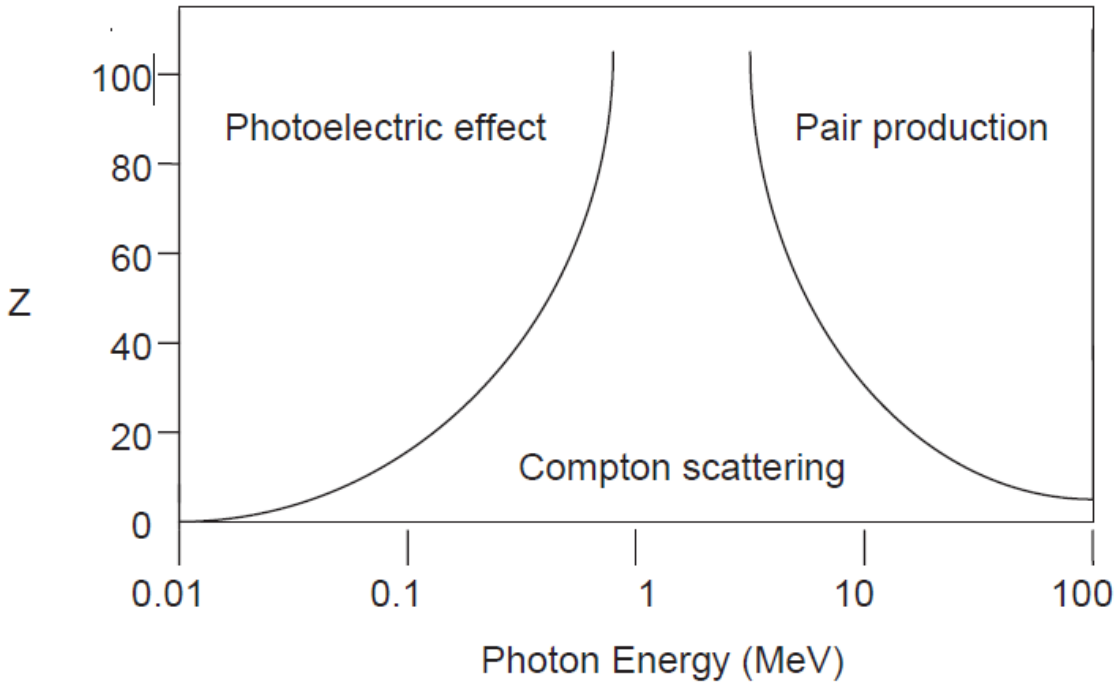

Figure 2-9: Interactions of gamma rays with matter (Kamunda, 2017).

2.6.2 Types of radiation detectors

Several methods and instruments are employed for radiation detection throughout the nuclear industry. These methods and instruments are able to measure the ionising radiation in samples. These instruments include: gas filled detectors, scintillation detectors and semi-conductor detectors.

The ionisation appears as electron-ion pairs in gas detectors and these charge carriers can be enticed and collected by electrodes (Khan, 2012). The ionised particles travels freely in gases as compared to solid or liquid. In gas detectors, gas fills the space between electrodes. The electric field is created through application of voltage by

potential difference between the electrodes. The positively charged gas atoms and electrons of the ion pair accelerates to cathode and anode respectively, causing an electric signal in the circuit.

The exposure of radiation interacts either in the wall of the chamber or directly in the filling-gas (Silva, 2019). Gas filled detectors are commonly used for the measurements of low energy electrons, ions and photons due to their poor stopping ability as detection medium for gamma rays (Onjefu, 2016). Gas filled detectors have very poor efficiency when compared to its counter parts.

Unlike gas-filled detectors, scintillation counters are used for both detection and measurement of ionising radiation. Scintillation counters are well-known for their ability to detect the fluorescent light (scintillation) emitted through excitation by nuclear particles (Kamunda, 2017) and when coupled to an amplifying device, the scintillations can be converted into electrical pulses. The response time for scintillation detectors is small. Although they have poor resolution, their efficiency of acquisition is high (Bode, 1998).

Semi-conductor detectors' unique properties have made an impact in the industry due to detection and measurement of radiation and they have a great energy resolution. These detectors have the capability to control their electronic conduction depending on the chemical structure, temperature, illumination, and presence of dopants. They are made from organic or inorganic materials (Silva, 2019). The solid semiconductor detectors are the preferred gamma ray detectors due to their high-energy resolution, good stability, exceptional timing characteristics and the simple approach of operating the detector (Ridha, 2016). Silicon and germanium (Ge) are the most commonly used materials for semiconductor detectors.

The Ge detectors are the preferred type as less energy is required for the creation of electric-pole pair (Kamunda, 2017). The Ge detectors are made of high purity material and have high density and atomic number. The high atomic number increases the gamma interaction probability of the detector. It requires only on average 2,6 eV of energy to create an electron-pole pair which gives the Ge detector a better energy resolution.

Figure 2-6 gives a clear view of the gamma ray spectrum measured by scintillation and semi-conductor detectors.

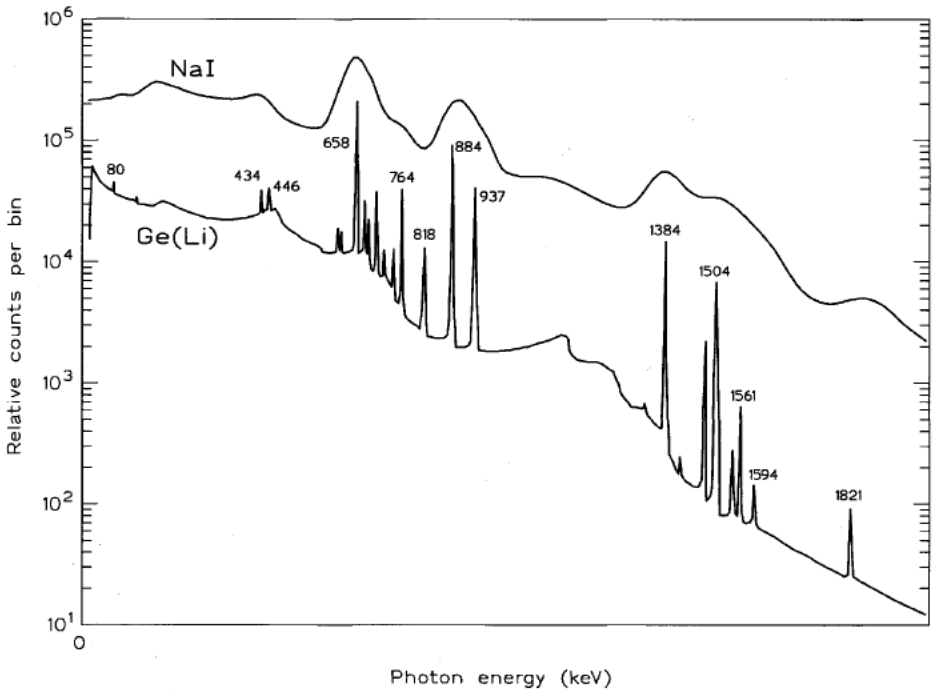

Figure 2-10: Different efficiency spectrums from scintillation (NaI) and semi-conductor Ge(Li) detectors (Ridha, 2016).

2.6.3 *In-Situ* Object Calibration Software and Multi Group Analysis for Uranium software

The *In-Situ* Object Calibration Software (ISOCS) is applied in several types of *in-situ* gamma ray spectrometry measurements such as isotopic mass of radionuclides, ^{235}U enrichment content, soil radioactivity and determination of radionuclide contamination amongst others (Grazadziel et al., 2017). This software has made it easy for IAEA inspectors to skip time-consuming steps for quantification and verification of nuclear materials.

The ISOCS software is employed by gamma–ray spectrometry. The spectrometry consists of a shielded detector, multichannel analyser and a computer that has software analyser. ISOCS software facilitates the generation of calibration efficiency curves without the use of standards. ISOCS software offers the capability to illustrate absolute efficiency curve for necessary energy range based on numerical simulation by using known or guessed geometry and chemical composition of measured samples. Sample geometry ranging from sphere, cylinder, box and complex shapes can easily be obtained using the ISOCS templates (Mirion Technologies, 2013).

The accurate detection and verification of uranium bearing materials is of high importance for nuclear safeguards, waste management and fighting illicit trafficking (Rüther and Zsigrai, 2015; Mirion Technologies, 2011). Measuring uranium has proven to be difficult in some instances whereby container wall thickness, container shapes, uranium chemical compositions differ and calibration is needed for each sample type (Abousahl et al., 1996). The Mutli-Group Analysis for Uranium (MGAU) code was developed to address the aforementioned limitations over traditional techniques of measuring ^{235}U enrichment in materials.

The MGAU code was designed to use the information from the intermediate energy region from 84 to 205 keV, that includes the gamma and X-rays (Mirion Technologies, 2011). The peaks found in this region have close energies and with better intensities compared to the 53 to 63 keV region that has very low energy and intensity gammas (Abousahl et al, 1996). This code uses the 90 to 94 keV region that has emissions of ^{235}U and ^{238}U for primary enrichment.

The 90 to 94 keV region has ^{238}U contribution from its daughter product (^{234}Th) emitting 92,38 and 92,80 keV while ^{235}U daughter product (^{231}Th) emits gamma ray 89,95 keV and two X-rays energies at 89,96 ($K\alpha_2$) and 93,35 ($K\alpha_1$) keV (Berlizov and Tryshyn, 2001). These peaks require special procedure to clarify the overlapping peaks due to the closeness of these peaks. MGAU code was developed with a response function to utilize when de-convoluting the overlapping peaks. The 185,7 keV of ^{235}U enrichment meter is also considered and/or used for enrichment. Some of the detected energy peaks are used to formulate a relative efficiency curve as a function of energy to eliminate the process of efficiency calibration before performing the measurements (Mirion Technologies, 2011).

For better results, MGAU code is best coupled with low energy germanium (LEGe) detector. The low energy peak shape and the resolution characteristics of this detector sets it apart (Mirion Technologies, 2011). While this code generates its own relative efficiency, it is also not time consuming and results are often ready in minutes but samples can be counted for longer.

2.6.4. Nuclear safeguards assaying techniques

The nuclear safeguards are applied by IAEA to member states to detect and deter diversion of nuclear material through verification and assaying techniques conducted by safeguards inspectors. The IAEA safeguards inspectors use a wide range of techniques to achieve this task. In order to maintain a valid safeguards system, there are three aspects that need to be placed and are as follows: physical control, accounting systems and measurement systems (Gavron, 2001). The assaying techniques form part of the measurement systems.

The assaying techniques used by safeguards inspectors are divided into destructive assay (DA) and non-destructive assay (NDA) (IAEA, 2011) which utilize different instruments. DA is defined as a process where a sample is broken down to measure the nuclear material content, isotopic composition and other chemical properties of the sample and it changes the physical form of the sample (Baker, 2018). This is contrasted with NDA, which is defined as the determination of the type and amount of nuclear material in an item without alteration of invasion of the item (Gavron, 2001).

The items that are mostly of concern when selecting a technique or instrument are the final products. The unburnt UF_4 samples are packaged, marking them as final products. The DA measurements would require that the unburnt samples be opened in order for small pieces to be taken for assaying but due to health and safety concerns, this type of assaying technique is ruled out. The NDA technique in the case of unburnt UF_4 is preferred, as it does not require the sample to be opened for assaying. For safety reasons, NDA is reliable because it obeys the three principles of ALARA, which are time, distance and shielding (IAEA, 2009b). The unburnts have high dose of radiation and using DA would exposure workers to radiation.

The DA techniques are mostly time consuming, as they require the sample pieces to be prepared before they could be assayed. In cases where samples are big and heterogeneous like the unburnts, the whole sample would require being grinded first to reach homogeneity and that destroys the original physical form of the sample. NDA measurements are usually rapid to acquire and reliable for samples that are heterogeneous (physically and chemically) (Gavron, 2001).

In cases where there are disputes with the results, it would be easier for NDA measurements to be redone (IAEA, 1977). Most NDA instruments are portable and they are easy to be operated on-site. If DA measurements need to be repeated, they would require sampling to be done and be sent for analysis. This could take time as some samples would need to be cured for certain periods and due to the size of DA instruments, transportation of equipment to the area of measurements may be challenging. Therefore, for analysing unburnt UF_4 NDA and its instruments are preferred. The DA can be utilized as well if there is a solution around issues of health and safety. The downside of only relying on NDA and not opening some samples is some drums may contain different nuclear materials to UF_4 when the IAEA inspectors try to verify it.

CHAPTER 3: MATERIALS AND METHODS

3.1 Sample description

Necsa used to run a uranium conversion plant to manufacture UF_6 for enrichment purposes and as a result, unburnt UF_4 wastes were generated through this process (Nangu et al., 2014). The ADU feed used for production of UF_4 and subsequently UF_6 had contamination from thorium. Therefore, the unburnt UF_4 had thorium concentrations due to contaminated ADU.

The UF_4 metal waste drums were enclosed in plastics overpacks/drums, which are shown in Figure 3-1. According to Nangu and others, only one drum has been opened due to the high level of radiation found in the sample (Nangu et al., 2014) and Figure 3-2 shows the opened over-pack.

Figure 3-1: The picture of UF_4 unburnt drums.

Figure 3-2: The picture of unburnt UF_4 open drum.

3.2 Mass and fill height measurements

3.2.1 Mass measurements

The quantity of the sample influences the results of the measurements and helps make better conclusions on mass dependent variables. The unburnt UF_4 material was measured to determine its quantity (sample mass) in the drums. The mass measurements were done using the Canberra rotating weighing table, connected to Sartorius reader. Gross, net and tare mass were measured.

The tare mass was determined using empty drums of the plastic overpack and 200 litre metal, same size as UF_4 unburnt drums. The tare mass was referred to as standard tare mass for measured values.

The gross mass measurements were conducted using the same method for tare mass measurements. The overpack drums containing the unburnt were weighed and the mass was recorded. The process was repeated for the 14 drums. The net mass of the samples was determined using equation (3.3):

$$\boldsymbol{W_N = W_G - W_T} \qquad (3.\ 1)$$

where:

W_N – net mass in grams (g)

W_G – gross weight (g)

W_T – tare weight (g)

3.2.2 Fill height and density measurements

The fill height of samples plays a critical role in identifying the volume and calculating the densities of the samples inside the drums. The methodology for measuring fill heights was adopted from (Nangu et al., 2014; Masemola et al., 2017) for this study. The ^{133}Ba transmission source was used to facilitate this procedure together with BEGe detector. The fill height measurements were conducted while the sample was on the rotating weigh scale for mass measurements.

The ^{133}Ba sealed point source has activity of 370 MBq and it produces gamma line at 356 keV. The ^{133}Ba transmission source was placed on a cart opposite BEGe detector with the sample in an adjacent position. Figure 3-3 demonstrates the positioning. According to the size of the 200-litre drum inside the plastic over-packs, the fill height of the unburnt UF_4 material should not exceed the 85 cm boundary line (Szuszkiewics, 2017).

Figure 3-3: The detector, sample and source position (left image) and sample and source position (right image).

The BEGe detector mouth was placed directly on the plastic over-pack to detect the ^{133}Ba peak at 356 keV. The ^{133}Ba transmission source was placed 35 cm away from the sample and was adjusted depending on the detection of the 356 keV peak. Measurements were done starting at the height of 0,5 cm going up. The fill height spectra were collected at five-minute intervals. The detection of 356 keV gamma line during the acquisition of the

spectrum gave a region for the estimated fill height of the drum, as the ^{133}Ba source does not transmit through the UF_4 unburnt material.

The drums that show no peak detection at 0,5 cm, the length of the drums is increased by 0,5 cm downwards, until a clear 356 keV peak gets detected. If there is still no detection at 12,70 cm of the drum, conclusion would then be made that the specific drum has no active uranium material as ^{133}Ba is sensitive to uranium and fill height will be noted as below detectable limit (BDL).

For drums that have detectable 356 keV peak, the fill height was determined by equation (3.2) and Figure 3-4 shows how the detector and transmission source work in determining the fill height of the UF_4 inside the drum. The doted red circle on the drum indicates the adjoining point of the transmission source and detector.

$$\boldsymbol{h_f = determined\ h_f - pallet\ height} \qquad (3.\ 2)$$

where:

h_f – fill height (cm)
$Pallet\ height$ – 12,70 cm

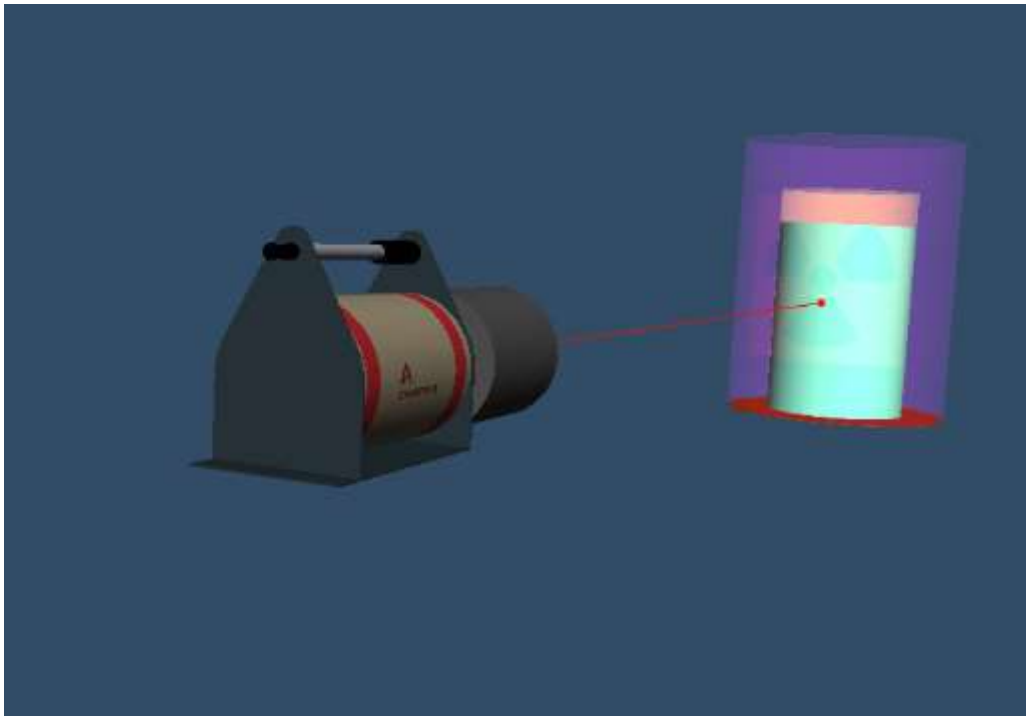

Figure 3-4: Simulated fill height diagram with the source behind the drum.

Once the fill height was determined, the density of the sample was calculated using equation (3.3). However, since the volume was unknown, equation (3.4) was used to determine volume using drum fill heights. The calculated mass in equation (3.1) was substituted in equation (3.3) together with calculated volume to determine the density.

$$\boldsymbol{\rho = \frac{m}{v}} \qquad (3.\ 3)$$

where:

ρ – density

m – mass

v – volume

$$\boldsymbol{v = h_f \times (\frac{\pi d^2}{4})} \qquad (3.\ 4)$$

where:

d – diameter

3.3 Activity and mass determination

3.3.1 Broad energy germanium detector

The broad energy germanium (BEGe) detector was used for measurement of gamma emitting radionuclides. The equipment used for gamma spectrometry consist of Canberra Model BE 2820 HPGe detector, with relative efficiency of 13%. The resolution: FWHM at 5.9 keV < 0.40 keV, FWHM at 122 keV <0.70 keV and FWHM at 1332 keV < 1.9 keV and thickness size: 20 mm diameter: 82 mm depth Aluminium end cap with intelligent preamplifier. It has a rather low background when compared to coaxial detectors.

3.3.2 Energy and efficiency calibration for BEGe detector

Energy calibration is determination of the relationship that exists between specific channel numbers and gamma ray energies. The energy calibration helps in identifying the radionuclides. In this study, the low-enriched uranium source covering energy range of 63.29 keV to 1001.3 keV was used. The system gain was set at 0.375 keV per channel.

The measured centroids peaks were plotted against the channel numbers on the MCA to generate energy calibration curve/plot. Figure 3-5 shows the energy calibration curve for BEGe detector. The relationship between energy and channel numbers is given in equation (3.5)

$$\boldsymbol{Energy = 1,010\ keV + 1,248Ch} \qquad (3.5)$$

where Ch is the channel number.

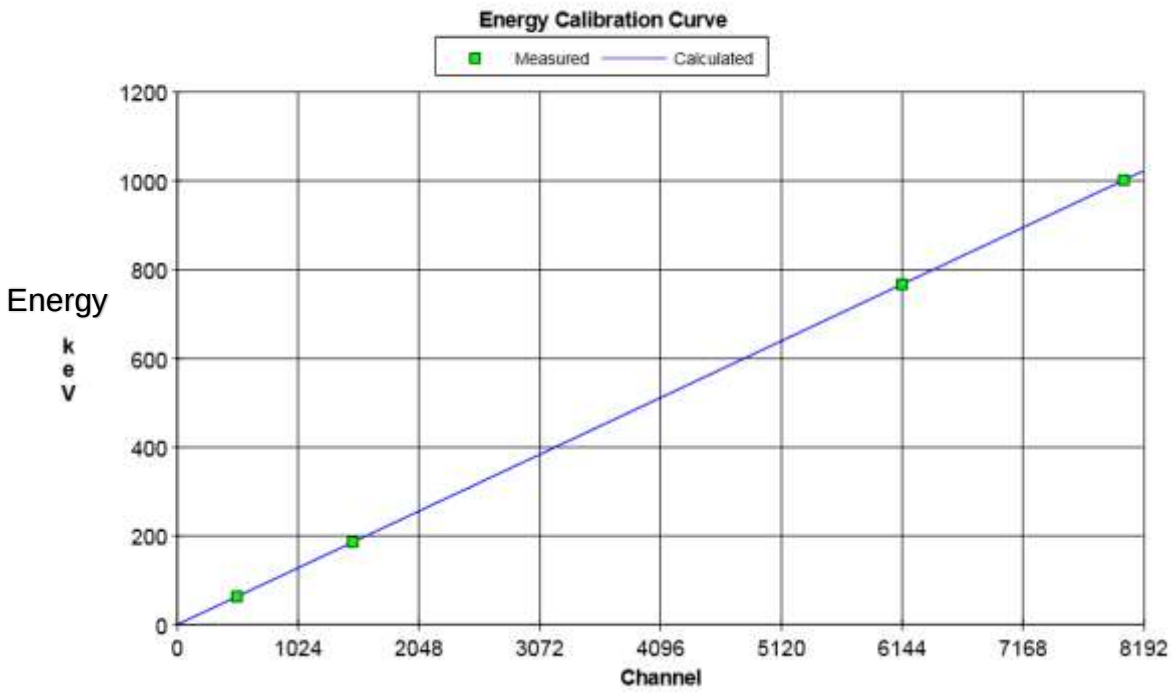

Figure 3-5: Energy calibration curve for BEGe detector.

The ISOCS calibration software was used to perform efficiency calibration using source and detector geometry composer. The efficiency calibration helps to interpret the spectrum in terms of activity to quantify radionuclides. The geometry template used was of cylinder shape and source parameters (size, density and source–detector distance) were entered into the ISOCS Calibration Software to generate an efficiency calibration. Each drum had its own efficiency calibration information as density and source-detector were not fixed. Figure 3–6 shows the efficiency calibration curve of the BEGe detector while equation (3.6) gives off the efficiency equation with 4th polynomial function.

$$\ln(Eff) = -1,946 + 1,197\ln(E) - 2,882\ln(E)^2 + 3,048\ln(E)^3 - 1,202ln(E)^4 \quad (3.\ 6)$$

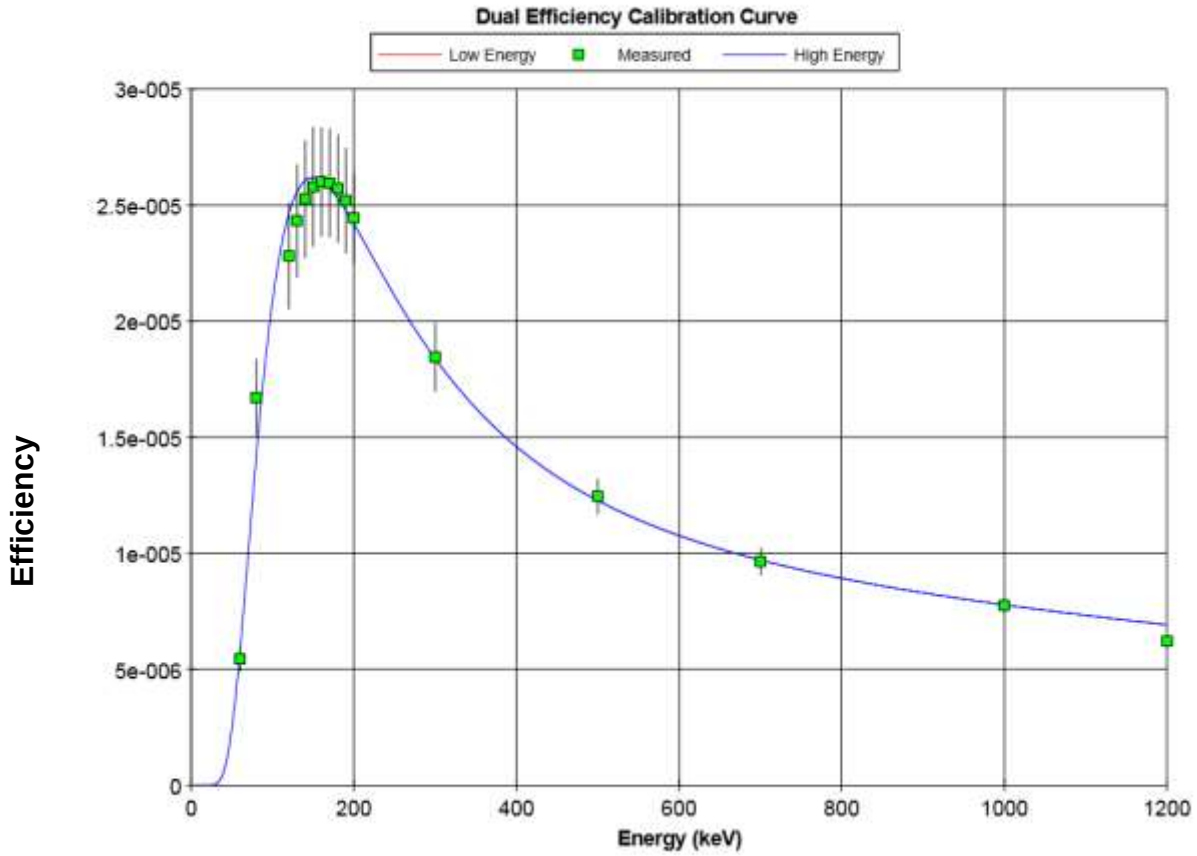

Figure 3-6: Efficiency calibration curve with fourth order polynomial function.

3.3.3 Activity and mass determination

To calculate the activity of ^{238}U in the unburnt UF_4, the daughter nuclides of ^{238}U series were used. The unburnt UF_4 are older than 20 years and the first two nuclides, ^{234}Th and ^{234m}Pa are in secular equilibrium with the series parent nuclide. Thorium-234 has a gamma line at 63.29 keV which is visible in most gamma ray spectra. This gamma line is found in high background region and its intensity and efficiency are usually low though there is less to no interference from other NORM nuclides. The other ^{234}Th gamma line lies at 92.6 keV and in this region, the detector's efficiency is relatively good and

background noise is lower. At this gamma line, there is interference of XK_{α} line of ^{231}Th (93.35 keV) from ^{235}U series.

The nuclide ^{234m}Pa, has two gamma lines at 766.36 keV and 1001.03 keV. These energies are found at a region with low detector efficiency and have low intensities. However, they are easily detected due to the low background at this region. The activity of ^{238}U was determined by calculating the weighted mean of the activity determined using ^{234}Th (63.29 keV) and ^{234m}Pa (766.36 keV and 1001.03 keV) gamma lines. The ^{234}Th 92.6 keV was not used due to the interference from ^{231}Th. The mass was calculated using equation (3.7):

$$m = \frac{A \times M_r}{N_A \times \lambda} \qquad (3.\ 7)$$

where:

A – activity; M_r – molar mass and N_A – Avogadro's constant.

The measurement of ^{235}U activity in the unburnt UF_4 was done using the 143.7 keV, 185.6 keV and 205.1 keV gamma lines. These energy lines are found in the high efficiency region of the detector and have strong intensity. The 98.44 keV X-ray peak was used to verify the presence of ^{235}U. The weighted mean of the activities determined using these gamma lines was used as the ^{235}U activity and subsequently the mass of ^{235}U was determined using equation (3.4). The enrichment estimation was done using equation (3.8):

$$\varepsilon_w = \frac{^{235}Umass}{^{235}U\ mass + {}^{238}U\ mass} \qquad (3.\ 8)$$

whereby:

ε_w = ^{235}U enrichment weight (g).

Thorium-232 is the parent radionuclide of the thorium decay series. This radionuclide cannot be determined directly through gamma ray spectroscopy due to its long half-life. Therefore, the daughter nuclides of ^{232}Th, namely ^{228}Ac (338.32 keV and 911.2 keV) and

^{212}Pb (238.6 keV) were used to determine the activity of ^{232}Th and subsequently the mass of thorium using equation (3.7).

CHAPTER 4: RESULTS AND DISCUSSION

Fifteen unburnt UF_4 drums were assayed using the BEGe detector. This detector analysed the samples using ISOCS and MGAU software to measure the mass content of ^{235}U, ^{238}U, ^{232}Th and the enrichment weight of ^{235}U.

4.1 Results of the Mass and fill height measurements

4.1.1 Mass measurements results

The Canberra scale was used to measure the mass of the UF_4 unburnt material in 200 litre drums. The mass measured plays a critical role in determining the densities of the UF_4 samples. Table 4-1 presents the mass measurement for 15 selected drums.

Table 4-1: The declared values versus measured values for UF_4 unburnt.

Sample ID	Declared		Measured	
	UF_4 gross mass (kg)	**UF_4 net mass (kg)**	**UF_4 gross mass (kg)**	**UF_4 net mass (kg)**
M1648	567.96	522.19	566.20	535.90
M1376	574.16	528.19	572.80	542.50
M1416	600.36	554.79	640.36	610.06
M1647	499.36	453.59	538.80	508.50
M919	358.81	317.24	347.00	316.70
UPN015	597.36	551.59	592.80	562.50
UPN014	725.96	679.99	719.40	689.10
M916	455.56	409.99	455.00	424.70
M596	189.20	143.23	188.60	158.30
M1031	439.56	393.99	438.40	408.10
M1646	557.76	510.99	557.40	527.10
M1675	624.96	578.79	624.40	594.10
M1403	667.76	624.19	667.40	637.10
M1498	180.30	134.53	230.20	199.90
M1649	589.76	543.59	588.80	558.50

An empty plastic overpack and 200 litre drum were measured and used as standard tare mass. The tare mass of 30,30 kg was recorded for all drums. The gross mass of the 15

drums ranged between 188,60 kg and 719,40 kg with gross average mass of 515,17 kg while net mass ranged from 158,30 kg to 689,10 kg with net average mass of 484,87 kg. The varying net mass of the unburnt suggest that the material was filled in without any specific criteria.

The difference in both gross and net weights can be observed in Figure 4-1. Drum UPN014 is the only drum that has gross weight over 700 kg. Apart from the mentioned drums, the results are slightly the same when compared to each other except drum M1498, M1416 and M1647. The difference in mass measured may indicate that the values declared were not done correct. Due to the lack of information and methodology on how the declared values were done, it can be assumed that that the measured values were correct and mass was measured twice during the acquisition of data collection to very the values.

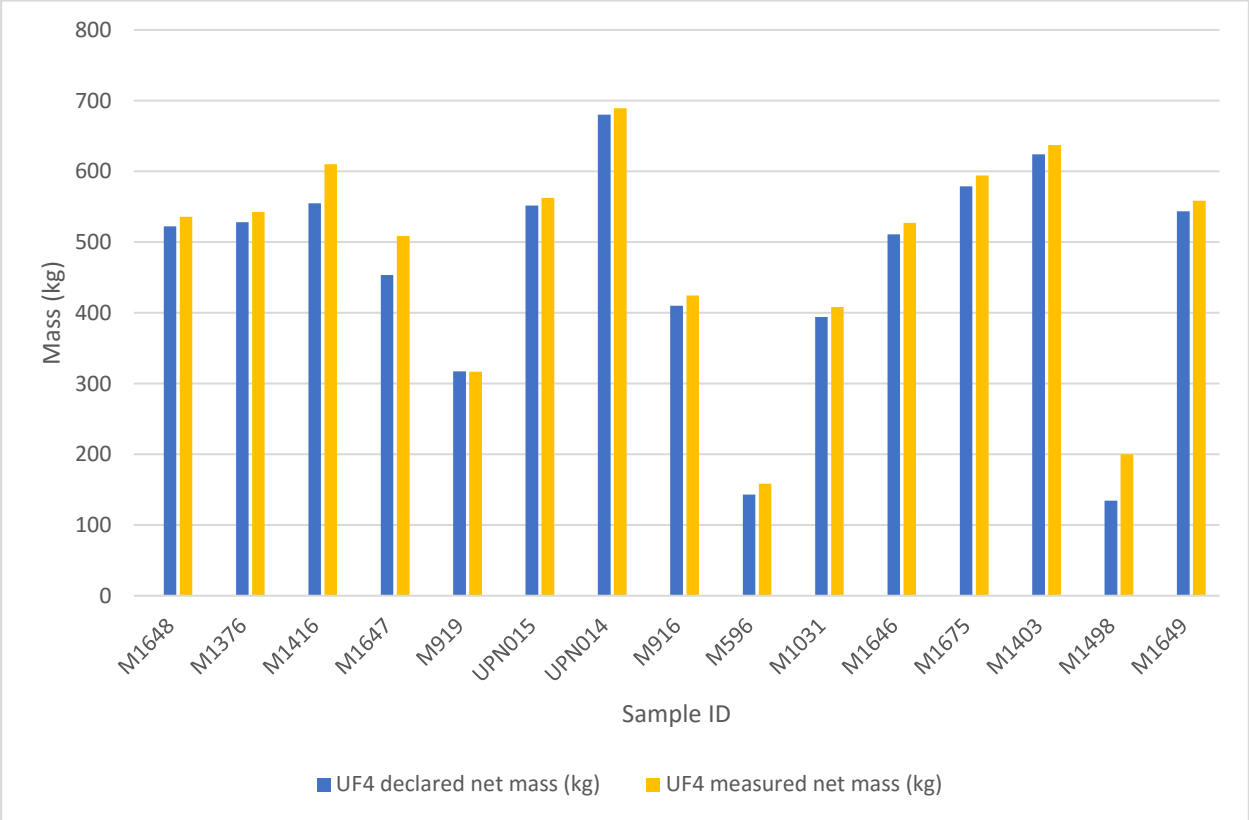

Figure 4-1: Graph presenting the declared and measured net masses.

4.1.2 Fill height measurements results

The fill height measurements play an important role in determining the volume and subsequently density of the UF_4 unburnt. The calculated volume therefore helps in determining the density of the drum used to store the unburnt material and for geometric composer of the ISOCS software for calibration. This information is important for the quantification of the unburnt, as they cannot be opened for safety reasons. The ^{133}Ba was used as transmission source for measuring the fill height of the drums with the aid of BEGe detector and ISOCS calibration software, and genie 2000 gamma acquisition and analysis software for spectrum acquisition.

The drums were measured from the bottom of the drum going up, with a source to sample distance of 35 cm and a sample to detector distance of 40 cm. The first visible peak detected was 356 keV, marked as an estimated region of the fill height of the drum measured. This is because the gamma photon from the ^{133}Ba source cannot penetrate the high density uranium if it is present in the sample. Figure 4-2 and 4-3 illustrates two spectra from drum M1647 at different heights. The spectrum on Figure 4-2 shows the prominent 356 keV peak at 92.5 cm from the bottom of the drum while Figure 4-2 shows a spectrum with less prominent peak at 356 keV at 91 cm taken from the bottom of the drum.

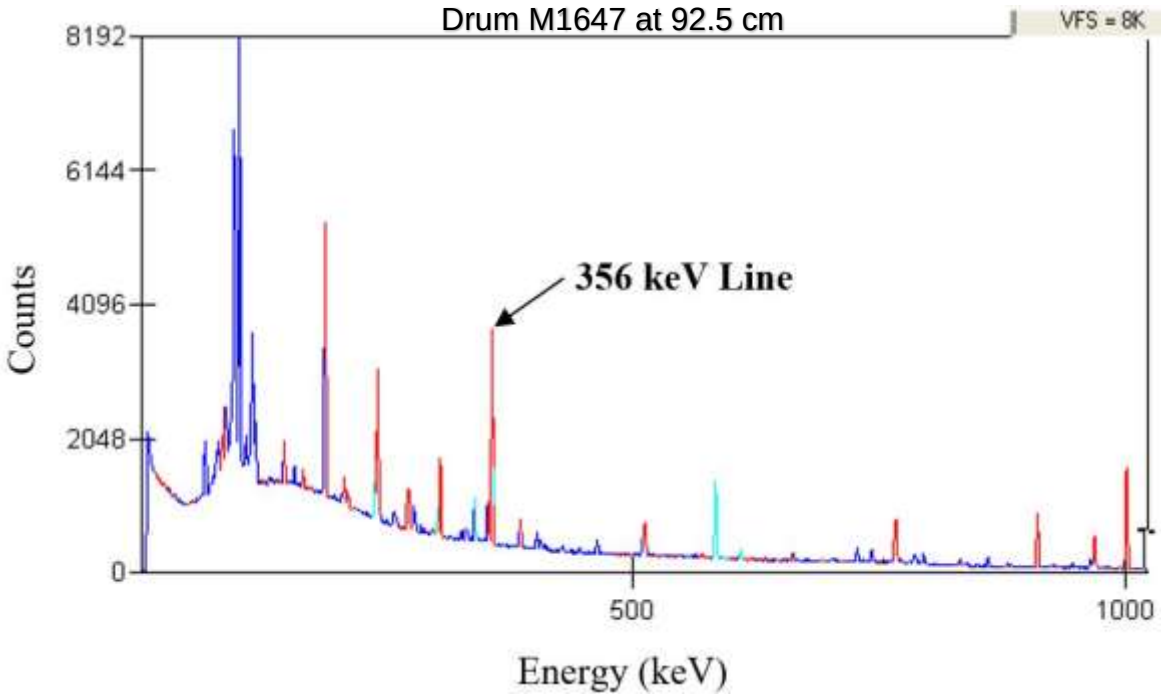

Figure 4 2: Fill height spectrum collect at 92.5 cm with prominent 356 keV peak.

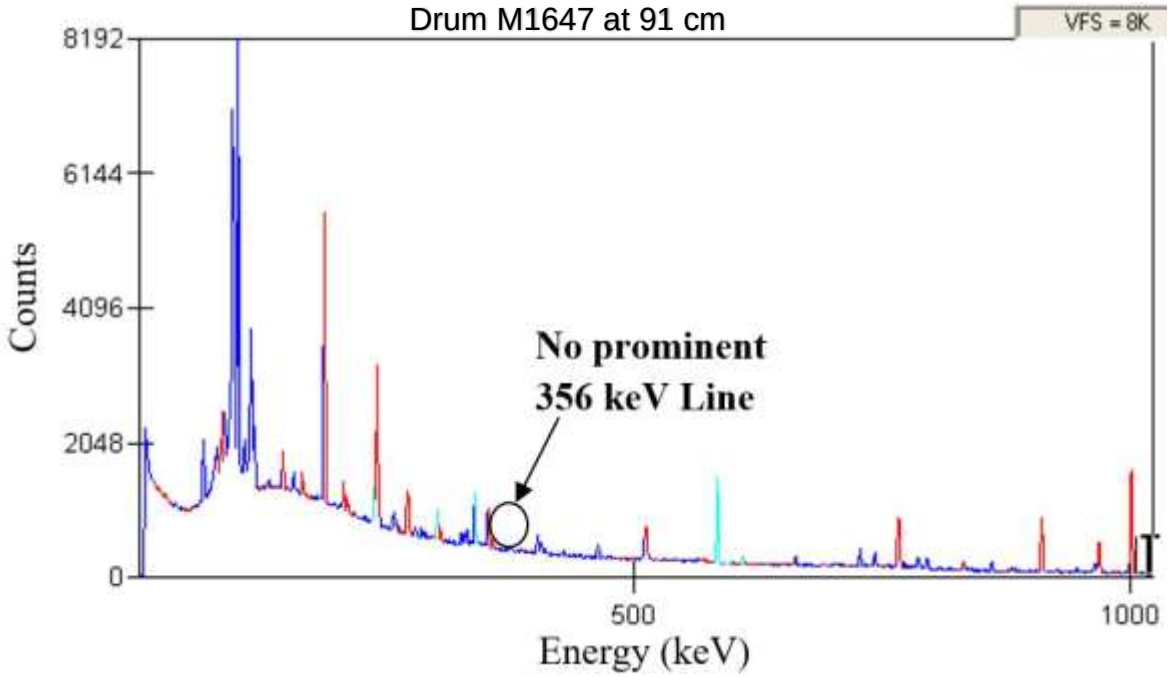

Figure 4-3: Fill height spectrum collected at 91 cm without prominent 356 keV peak.

The spectrum in Figure 4-2 shows the penetration of the ^{133}Ba source through the UF_4 unburnt drum hence the prominent 356 keV peak. The gamma photons emitted by the

^{133}Ba source cannot penetrate the UF_4 material. The UF4 acts as a shielding material, and this is presented in Figure 4-3. Due to the above mentioned reasons, the fill height values of the unburnt drums are determined through the acquired spectrums.

Table 4- 2: Fill height measurements and densities of the UF_4 unburnts samples.

Sample ID	Net mass (kg)	Fill height (cm)	Volume (cm^3)	Density (g/cm^3)
M1648	535.90	85.00	216527.09	2.47
M1376	546.60	75.80	192880.41	2.83
M1416	614.60	70.80	179927.36	3.41
M1647	508.50	84.50	215247.38	2.36
M919	322.10	61.90	157404.44	2.05
UPN015	562.50	85.00	216527.09	2.60
UPN014	689.10	83.10	211664.19	3.26
M916	424.70	85.00	216527.09	1.96
M596	163.70	52.80	134113.70	1.22
M1031	412.20	60.30	153309.37	2.69
M1646	527.10	85.00	216527.09	2.43
M1675	598.20	78.10	198867.08	3.01
M1403	637.10	83.10	212687.96	3.00
M1498	205.30	60.80	154589.08	1.33
M1649	558.50	81.70	208081.00	2.68

Fifteen drums were selected for measurements and fill height measurements were performed on all drums and their results are presented in Table 4-2. From the data collected, the fill heights ranged between 52.40 cm and 85.00 cm as shown in Table 4-2 with source – sample distance at 35.00 cm. The UF_4 unburnt drums are reported to have high radiation dose by the storage facility, as such, the drums were measured at detector distance of 40.00 cm for this study.

The fill height data has a difference of 32.20 cm and this could be due to the following reasons:

- some drums contain UF_4 as moist powder and/or dry hardened cement
- the UF_4 material in some drums was compacted

According to the fill height data collected, the fill height is not dependent on the net weight of the UF_4 material. Drum M1403 has net weight of 637.10 kg with fill height of 83.50 cm as compared to drum M1646 with 527.10 kg net weight and maximum fill height of 85.00 cm. From this extracted data, it shows that drum M1646 is 110 kg less than drum M1403 and yet its fill height is higher. This indicates that, drums that have high net weight with low fill height may have had the unburnt compacted during the packaging process.

Volume and density measurements are also presented in Table 4-2 and a wide range of information from literature suggested that density of the UF_4 in crystal form is 6.7 g/cm^3 and density of the UF_4 in bulk form is between 1.8 – 4.5 g/cm^3 (Bronson et al., 2007). The calculated density ranges between 1.22 and 3.41 g/cm^3. Out of the fifteen drums measured, only thirteen drums fit the density range reported in literature and the two others have density below 1.8 g/cm^3. The drums that have density that is below the standard density value of UF_4 could be due to the presence of ^{232}Th and fluorine and other chemicals used for UF_6 production process.

Densities of the samples do not follow any specific trend. Drum M916 has density of 1.96 g/cm^3 with fill height of 85.00 cm and drum M1031 has density of 2.69 g/cm^3 with a relatively low fill height of 60.30 cm. These drums have mass of 424.7 kg and 412.2 kg, respectively. However, their measured densities are not in the same range, with one being out of range based on the literature. The possible explanation to this could be that the material inside these drums is not homogenous hence the varying fill heights and densities.

4.2 Results of Uranium isotopic mass measurements

The isotopic mass content of ^{235}U and ^{238}U were measured using BEGe detector with characterised Inspector 2000 (Canberra Industries Inc) with ISOCS software. The measurements were done at a live time of 3600 seconds. Figure 4-4 and Table 4-3 shows the spectrum with prominent gamma-lines of uranium and thorium daughter nuclides.

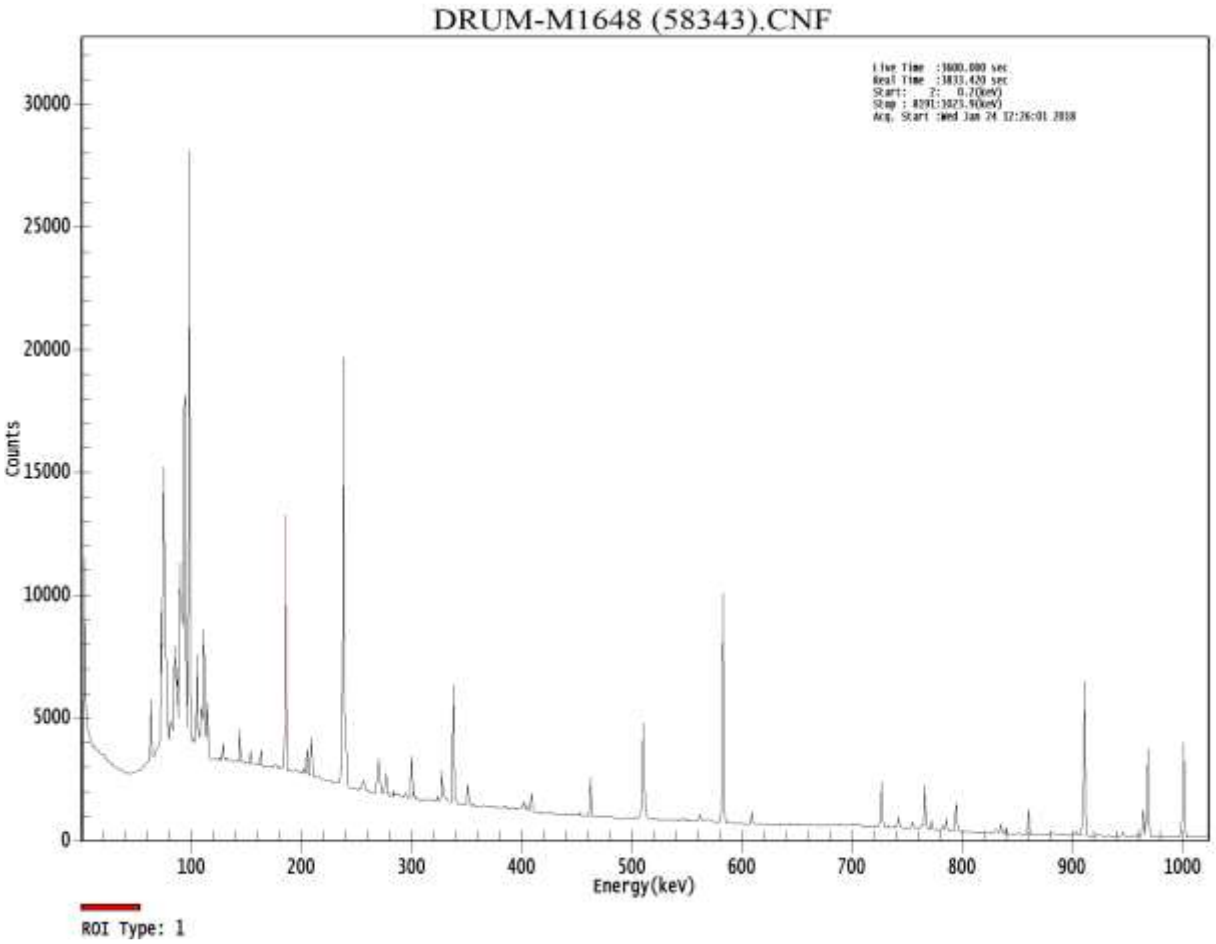

Figure 4-4: Gamma-ray spectrum of drum M1648 obtained using BEGe detector.

In Figure 4-4 the prominent gamma lines for ^{235}U (143.7, 163.4 and 185.6 keV), ^{238}U (63.29; 766.36 and 1001.1 keV) which belongs to ^{234}U and ^{234m}Pa, daughter nuclides of ^{238}U and ^{232}Th (238.63; 338.32 and 911.20 keV) which belongs to ^{212}Pb and ^{228}Ac, daughters of ^{232}Th are shown.

Table 4-3: ^{235}U and ^{238}U isotopic mass analysed by ISOCS software with associated uncertainties.

Drum ID	^{238}U mass (kg)	^{235}U mass (kg)	^{232}Th mass (kg)	^{235}U enrichment (wt. %)
M1376	1.900±0.105	0.020±0.000	BDL	1.054±0.052
M1403	1.895±0.096	0.013±0.000	0.801±0.022	0.692±0.048
M1031	0.742±0.044	0.007±0.003	0.313±0.009	0.942±0.021
M1416	1.583±0.090	0.020±0.003	0.222±0.007	1.271±0.044
M1498	2.637±0.103	0.019±0.003	0.227±0.007	0.701±0.050
M1646	0.945±0.069	0.011±0.003	0.817±0.033	1.158±0.033
M1647	1.783±0.094	0.021±0.003	0.407±0.011	1.138±0.046
M1648	1.288±0.076	0.016±0.001	1.125±0.028	1.245±0.038
M1649	1.132±0.063	0.012±0.003	0.662±0.015	1.085±0.030
M1675	0.882±0.057	0.012±0.003	0.559±0.015	1.358±0.027
M916	0.884±0.049	0.009±0.000	0.434±0.012	0.969±0.024
M919	2.351±0.090	0.011±0.003	0.989±0.026	0.436±0.044
UPN014	2.060±0.112	0.024±0.003	0.434±0.012	1.140±0.055
UPN015	1.817±0.098	0.022±0.003	0.812±0.021	1.194±0.048
M596	BDL	BDL	1.097±0.031	BDL

According to the results presented in Table 4-3, the ISOCS software detected the uranium composition successfully except from M596 which had uranium content that was below detection limit of the BEGe detector. The ^{238}U mass ranged between 0.742±0.044 – 2.637±0.103 kg with average of 1.472±0.076 kg and M1498 had the highest ^{238}U mass. Although M596 had a mass of 158.30 kg, the material had less counts for ISOCS to detect any uranium mass/daughter nuclides activities. The representation of the figures in bar graph are presented in Figure 4-5.

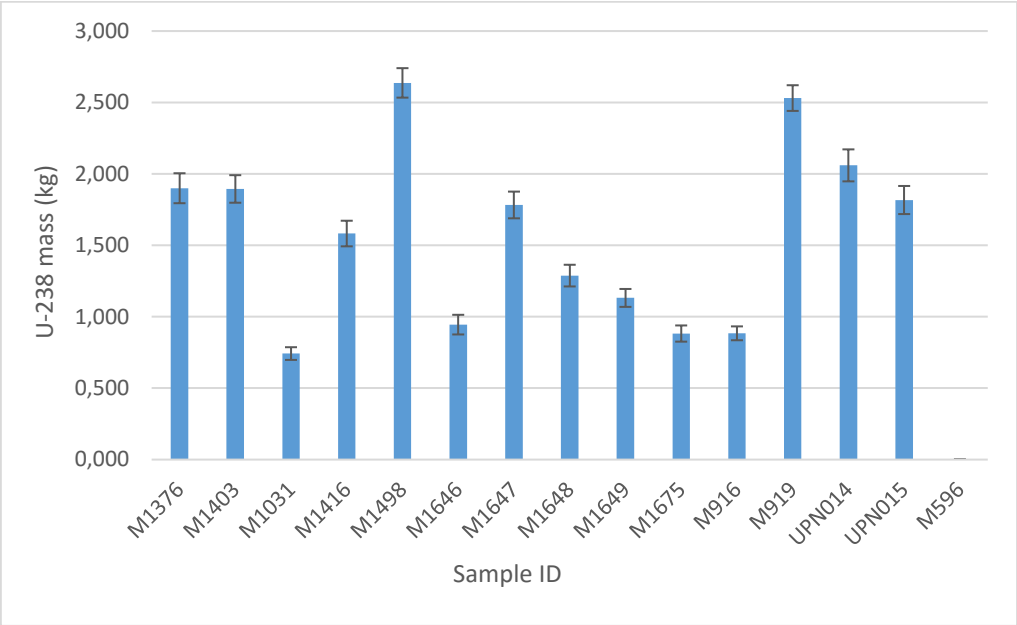

Figure 4-5: Graph showing the ^{238}U isotopic mass in UF_4 unburnt drums.

The ^{235}U mass ranged from 0.007±0.003 to 0.024±0.003 kg with average of 0.014±0.002 kg and UPN014 had the highest mass. The failure of software in detecting the ^{235}U and extrapolating a spectrum, justifies that M596 had no active uranium material. Figure 4-6 shows the ^{235}U isotopic mass.

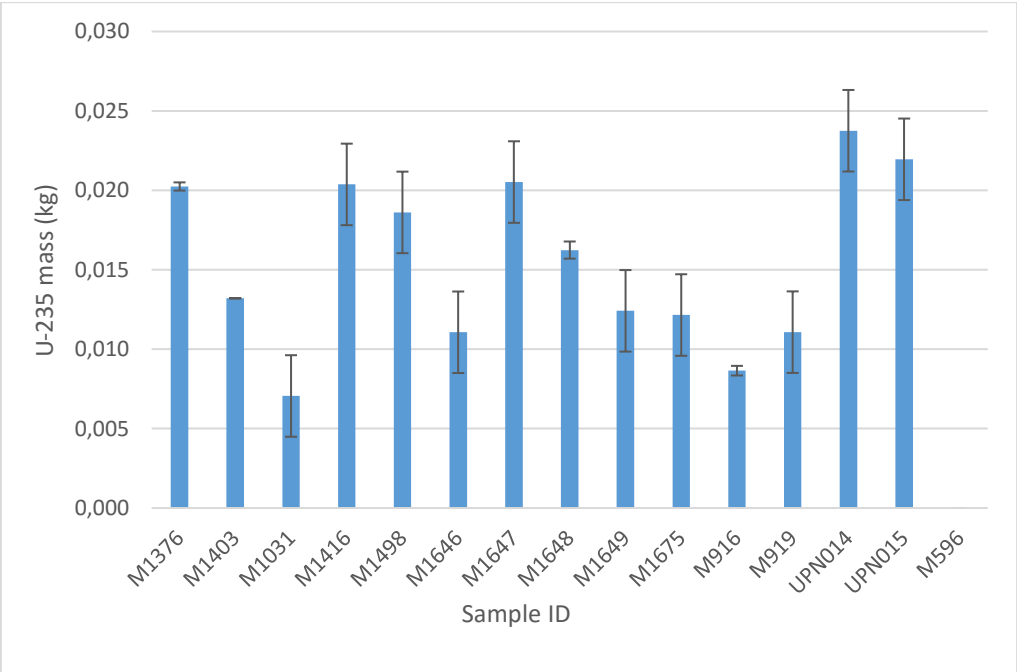

Figure 4-6: Graph showing the ^{235}U isotopic mass in UF_4 unburnts drums.

Using the mass of ^{235}U and ^{238}U in Table 4-3, the enrichment estimation of ^{235}U for the ISOCS software was determined using equation (3.5). The estimated enrichment ranged between 0.436±0.044 to 1.358±0.027 wt.% with an average of 0.59±0.037 wt.%. M596 had no enrichment results due to no uranium detection while M1675 had the highest enrichment estimate at 1.358±0.027 wt.%. Figure 4-7 shows the comparison of the calculated ^{235}U enrichment estimates against the facility declared 0.711 wt.% enrichment of ^{235}U. It was assumed that the declared enrichment was in natural abundance (0.711%) which makes the declared value not certified. The differences observed were because it was the first time the actual enrichment measured were done. Therefore, the assumption made that declared enrichment was 0.711% was not correct according to the study.

Sample M1403, M1498 and M919 have enrichment below 0.711 wt.%, which are low in this case. Thorium content in the aforementioned samples is relatively higher as presented in Table 4-3. The presence of intense $K\alpha_1$ X-ray at 93.347 keV from thorium affects the spectrum ability to separate it from 93.650 keV from uranium. As such, the enrichment estimation of ^{235}U often gets compromised when the sample have thorium in great content.

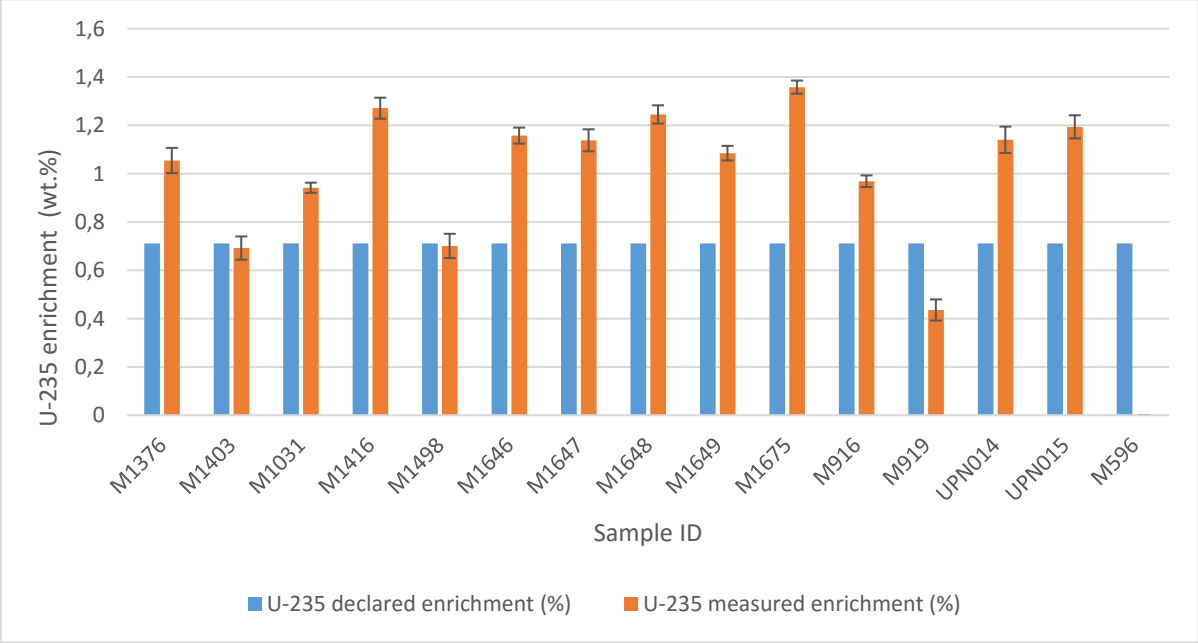

Figure 4-7: ISOCS and declared ^{235}U enrichment comparison.

The measurement of thorium content was successful in 14 drums with only M1376 not detected. The ^{232}Th mass content ranged from 0.222±0.007 kg to 1.125±0.028 kg. The results indicate and provide proof that UF_4 unburnt are a mixture of naturally occurring radionuclides. M1648 has relatively the highest concentration of ^{232}Th and this could be because ADU in the sample is high. Figure 4-8 presents the ^{232}Th masses.

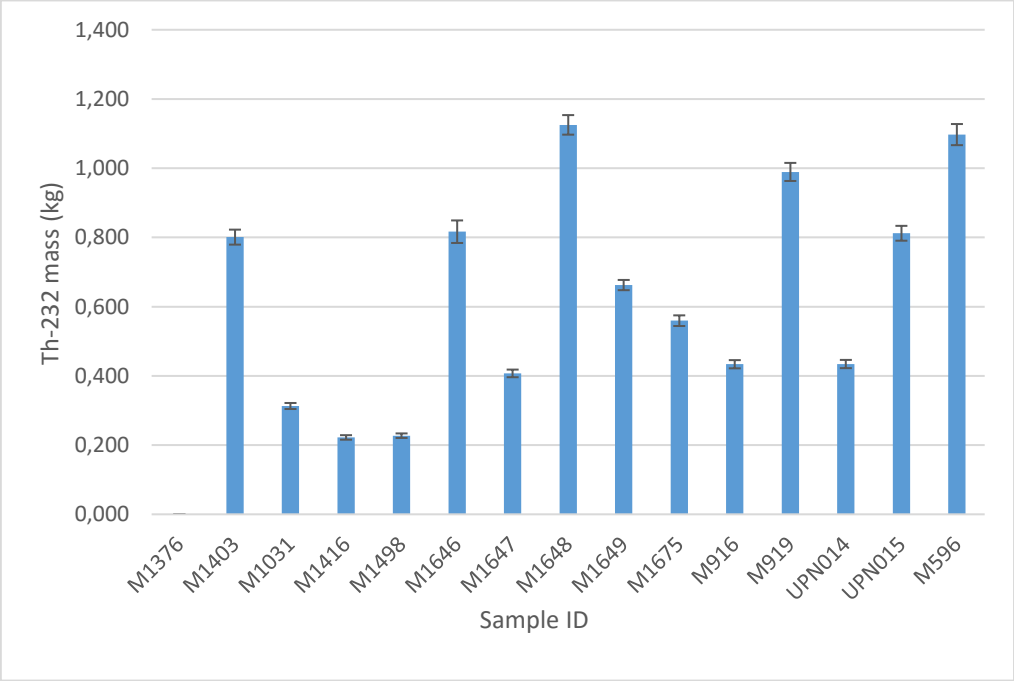

Figure 4-8: Graph showing ^{232}Th content in UF_4 unburnt.

From the uranium isotopic mass presented in this section, it is clear that the unburnt have considerable elementary mass of natural uranium except in M596. The isotopic content of ^{238}U shows the relationship that exist at natural state of this isotope while presence of ^{232}Th justifies that the sample material is NORM. However, even though the same plant was used to generate the UF_4 unburnt the distribution of the uranium was not homogenous. Different loads of UF_4 concentrations were used, which could have yielded uneven distribution. The ^{235}U enrichment estimates depend solely on the uranium isotopic mass. The enrichment estimates are below 1.5 wt.% and this is due to low isotopic mass yield.

4.3 ^{235}U enrichment estimates by MGAU software

^{235}U enrichment estimate results were generated using BEGe with InSpector 2000 (Canberra Industries Inc) with MGAU V4.2 and MGAU V4.3 software. Figure 4-9 illustrates the counting geometry for measurements of the unburnt through BEGe detector while Figure 4-10 shows a generic spectrum generated by MGAU V4.3 code.

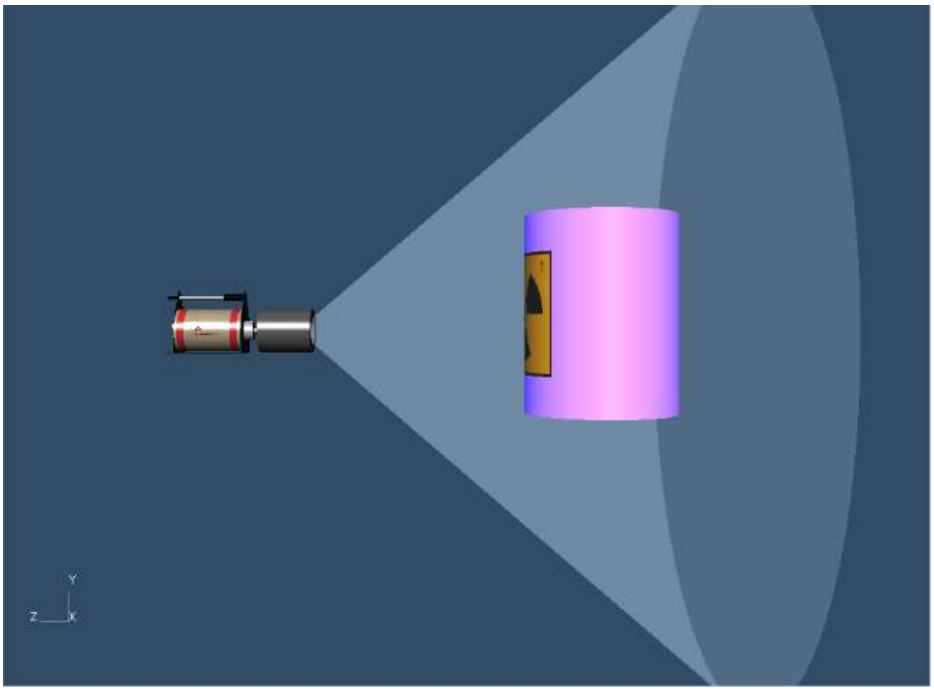

Figure 4-9: BEGe counting geometry.

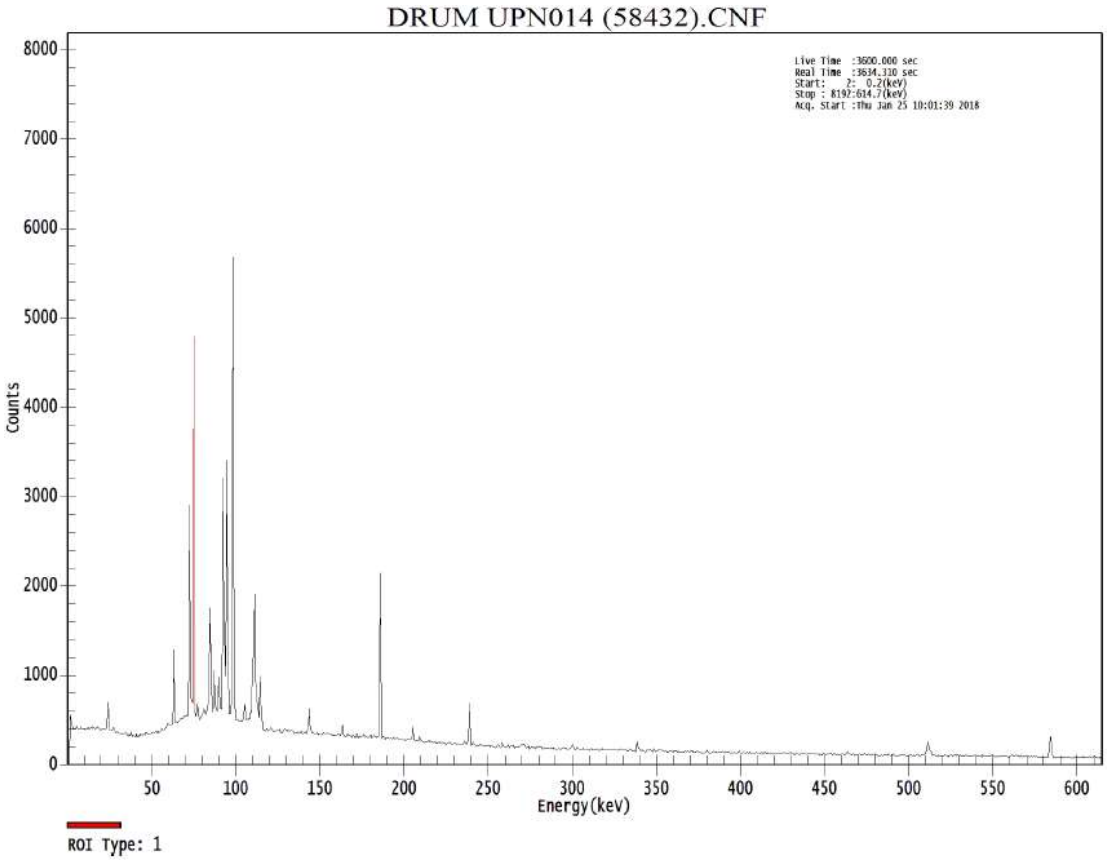

Figure 4-10: Spectrum of UPN014 using MGAU V4.3 software.

This section presents and discuss results of ^{235}U enrichment and Table 4-4 presents the UF_4 unburnt results measured at 60-minutes live time with the declared enrichment values.

Table 4-4: ^{235}U enrichment estimates by MGAU V4.2 and MGAU V4.3 software with associated uncertainties.

Sample ID	Declared ^{235}U enrichment (wt.%)	MGAU V4.2 (wt.%)	MGAU V4.3 (wt.%)
M1648	0.711	0.871±0.101	0.905±0.102
M1376	0.711	0.754±0.056	0.752±0.045
M1416	0.711	0.612±0.084	0.766±0.082
M1647	0.711	1.353±0.105	1.635±0.121
M919	0.711	0.589±0.120	0.535±0.149
UPN015	0.711	1.194±0.087	1.059±0.110

UPN014	0.711	0.753±0.082	0.822±0.077
M916	0.711	0.706±0.112	0.634±0.135
M596	0.711	BDL	BDL
M1031	0.711	0.896±0.119	0.658±0.134
M1646	0.711	0.782±0.127	1.167±0.169
M1675	0.711	1.438±0.115	0.860±0.105
M1403	0.711	0.902±0.096	0.662±0.105
M1498	0.711	0.532±0.074	0.721±0.074
M1649	0.711	0.941±0.107	0.940±0.105

The MGAU V4.2 enrichment results ranged between 0.532±0.074 and 1.438±0.115 wt.% with average enrichment of 0.822±0.092 wt.%. However, M1647, UPN015 and M1675 showed considerately high enrichment values as compared to the 0.711 wt.% with errors reported at 1–sigma. Drums that recorded ^{235}U enrichment value closer to the standard reference point had dead time below 4.0 %. The ^{235}U enrichment for M596 was undetected. From Table 4-3, M596 registered 0.00 kg of ^{235}U from ISOCS measurements.

The MGAU V4.3 was utilised for analysis of enrichment values of ^{235}U and from 15 measurements done, only M596 had enrichment below detection. The MGAU V4.3 enrichment results ranged between 0.535±0.149 to 1.635±0.121 wt.% with average enrichment of 0.808±0.100 wt.%. The activities of the major ^{235}U gamma lines were also undetected. M1647 had the highest enrichment estimate while M919 had the lowest. Figure 4-11 represents the comparison between the two MGAU versions.

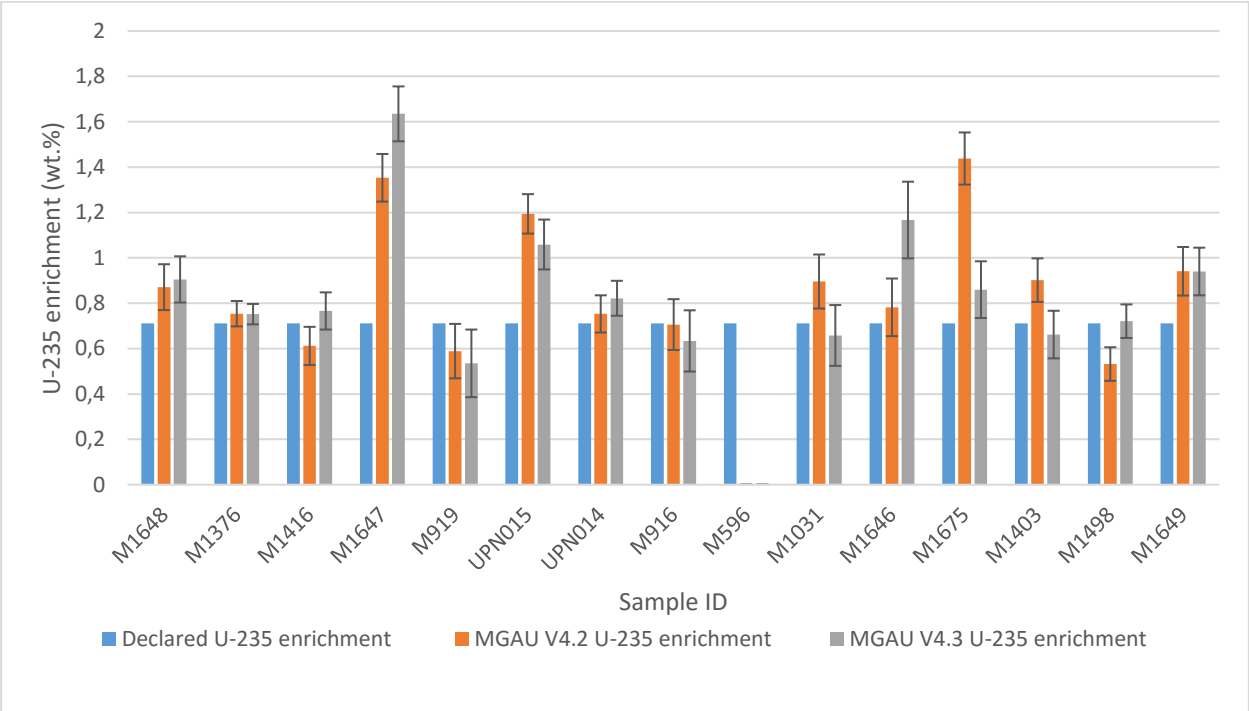

Figure 4-11: Graph showing ^{235}U Enrichment comparison using MGAU software.

The ^{235}U enrichment estimates analysed by both MGAU versions shows no statistical significance between the results. The average of MGAU V4.3 is closer to the declared value than MGAU V4.2.

CHAPTER 5: CONCLUSION AND RECOMMENDATIONS

5.1 Conclusion

The aim of the study was to characterize the UF_4 (unburnts) in terms of gross mass, net mass, fill heights, material density, enrichment level, ^{232}Th mass, ^{235}U mass and ^{238}U mass. This study was motivated by the need to quantify the UF_4 (unburnt) measurements that are to be declared to the IAEA. The UF_4 unburnt samples were stored at the interim storage facility, while studies were done on ways to quantify them. High purity germanium detector was used to measure the isotopic mass of ^{232}Th, ^{235}U and ^{238}U. The enrichment of ^{235}U was determined from the calculated masses of ^{235}U and ^{238}U in the 15 selected UF_4 unburnt drums.

The density of the UF_4 unburnts was determined through fill height and mass measurements. The densities determined ranged between 1.22 and 3.26 g/cm^3 as compared to the density of 1.8 – 4.5 g/cm3 reported in literature (Bronson et al., 2007). From the calculated densities, it was observed that the UF_4 unburnts are not homogenous as some had densities below 1.8 g/cm^3.

The determination of uranium isotopic mass and enrichment using gamma spectrometry and ISOCS calibration system was successful. The isotopic mass of ^{238}U and ^{235}U was determined in 14 drums and they ranged from 0.742±0.044 kg to 1.900±0.105 and 0.007±0.003 kg to 0.024±0.003 kg, respectively. However, there was no quantifiable amount of uranium that could be detected from drum M596. The mass of ^{232}Th was measured successfully in the 15 drums but the thorium content in drum M1376 was below the detectable limit. The mass of ^{232}Th ranged between 0.222±0.007 kg and 1.125±0.028 kg. Moreover, the enrichment of ^{235}U was determined using the same system. The enrichment ranged from 0.436±0.044 wt.% to 1.358±0.027 wt.%. The measured enrichment levels were higher than the declared value of 0.711 wt.%.

The MGAU was also used to estimate the enrichment of ^{235}U. Two versions of the software were used, version MGAU V4.2 and MGAU V4.3. The ^{235}U enrichment values determined using MGAU V4.2 ranged between 0.532±0.074 and 1.438±0.115 wt.% while those determined with MGAU V4.3 ranged between 0.535±0.149 and 1.635±0.121 wt.%. The gamma spectrometry system running ISOCS and both MGAU codes confirmed that the level of uranium in drum M596 was below the detectable limit.

The BEGe detector, using three different software measured the unburnt effectively and mass contents of ^{238}U, ^{235}U and ^{232}Th and ^{235}U enrichment were measured successfully. The measured ^{235}U enrichment are in close range to the declared value.

5.2 Recommendations

For future studies, the following recommendations should be considered;

- using X-ray scanner to determine the sample fill height in drums as distribution of the material may not be even and
- checking how the modifications done on MGAU V4.3 affect the results, as the results do not show significant variance from MGAU V4.2.

REFERENCES

Abousahl, A., Michiels, A., Bickel, M., Gunnink, R., and Verplancke, J., 1996. Applicability and limits of the MGAU code for the determination of the enrichment of uranium samples. Nuclear instruments and methods in physics research, Volume 368, pp 443-448.

Daryl Kimball, 2019. The nuclear non-proliferation treaty at glance, Arms Control Association . [Online] Available at: https://www.armscontrol.org/factsheets/nptfact [Accessed 10 October 2019].

ANL, 2001. Human health fact sheet: Thorium. [Online] Available at: http://hpschapters.org/northcarolina/NSDS/thorium.pdf [Accessed 17 August 2017].

Awan, I.Z. and Khan, A.Q., 2015. Uranium – The Element: Its Occurrence and Uses. J.Chem.Soc.Pak., Volume 37, pp. 1056-1080.

Baker, M.C., 2018. Nuclear Safeguards and Proliferation of Nuclear Weapons Materials. Encyclopedia of Sustainability Science and Technology Series. New York: Springer.

Berlizov, A.N., and Tryshyn, V.V., 2001. Study of the MGAU applicability to accurate isotopic characterisation of uranium samples. Ukraine.

Bharath-Ram, K., Eberhard, A., Myers, M., Sellschop, F., and Webster, R., 1997. Atomic Energy Corporation Review. Final report. [Online] Available at: https://fas.org/nuke/guide/rsa/agency/aecpg1.htm [Accessed 15 November 2018].

Bronson, F., Atrashkevich, V., Geurkov, G., and Young, B., 2007. Probablistic uncertainty estimator for gamma-spectroscopy measurement, Meriden CT: Canberra Industries.

Bredell, P.J., 1990. Uranium conversion and enrichment (INIS-XA-N--169). International Atomic Energy Agency (IAEA).

Cember, H. and Johnson, T. E., 2009. Introduction to Health Physics. New York, McGraw-Hill.

Cherry, S.R., Sorenson, J.A., and Phelps, M.E., 2012. Chapter 4 - Decay of Radioactivity. Physics in Nuclear Medicine, 4th Edition. Saunders.

Dewji, S., 2014. Safeguards assessment of gamma ray detection for process monitoring at natural uranium conversion facilities, Georgia: Georgia Institute of Technology.

Dlamini, T.C., 2014. Radionuclides and toxic elements transfer from the Princess Dump to the surrounding vegetation in Roodepoort South Africa: Potential radiological and toxicological impact on humans. Mafikeng, North-West U niversity.

Doo, J., Hurt, R., Fagerholm, R. and Tuley, N., 2003. Safeguards approach for natural uranium conversion plants. Phoenix, s.n.

Erpenbeck, H., 2017. Safeguarding the nuclear fuel cycle: mining, milling, and conversion. Los Alamos National Laboratory,Tennessee, USA.

Eskom, 2018. Eskom: Services - Electricity generation. [Online] Available at: www.eskom.co.za/Whatweredoing/ElectricityGeneration/KoebergNuclearPowerStation/Pages/Koeberg_Power_Station.aspx [Accessed 25 October 2018].

Frimmel, E., Schedel, S., and Brätz, H., 2014. Uraninite chemistry as forensic tool for provenance analysis. Applied Geochemistry. Volume 42, pp. 104-121.

Gavron, A., 2001. Nondestructive assay techniques applied to nuclear materials. New Mexico: LANL.

Gilmore, G., 2008. Practical gamma-ray specrometry. 2nd ed. Chichester: John Wiley & Sons Ltd.

Grazadziel, D., Kozak, K., Mazur, J. and and Mroczek, M., 2017. Application of ISOCS system in the laboratory efficiency calibration. Environmental Radiaoctivity. Volume 188, pp. 95-99.

Hyde, E. K., 1960. The Radiochemistry of Thorium. In: ENERGY, U. D. O. (ed.). California.

IAEA, 1965. Information circulation 70, Vienna: IAEA

IAEA, 1967. Information circulation 98, Vienna: IAEA

IAEA, 1970. Information circulation 140, Vienna: IAEA.

IAEA, 1972. Information circulation 153, Vienna: IAEA

IAEA, 1977. The international scope of safeguards. Volume 19(5). Vienna: IAEA.

IAEA, 1991. Information Circulation 394, Vienna: IAEA.

IAEA, 1999. Minimization of waste from uranium purification, enrichment and fuel fabrication. Tecdoc-1115 ed. Vienna: IAEA.

IAEA, 2005. Thorium Fuel Cycle - Potential Benefits and Challenges, IAEA-Tecdoc-1450, Vienna: IAEA.

IAEA, 2009a. Safeguards measures applicable in conversion plants processing natural uranium (Policy Paper 18), Vienna: s.n.

IAEA, 2009b. The nuclear fuel cycle information system: A directory of nuclear fuel cycle facilities.. Tecdoc-1613 ed. Vienna: IAEA.

IAEA, 2011. Safeguards techniques and equipments: 2011 Edition. International nuclear verification series 1 (2nd rev). Vienna: IAEA.

IAEA, 2015. Safeguards: Serving nuclear non-proliferation. Vienna: IAEA.

IAEA, 2018. Status and Trends in Spent Fuel and Radioactive Waste Management, Nuclear Energy Series No. NW-T-1.14. Vienna: IAEA

IAEA, 2019a. Non-proliferation treaty, 60 years IAEA atoms for peace and development. [Online] Available at: https://www.iaea.org/topics/non-proliferation-treaty [Accessed 20 September 2019].

IAEA, 2019b. Safeguards explained. [Online] Available at: https://www.iaea.org/topics/safeguards-explained [Accessed 15 October 2019]

Kamunda, C., 2017. Human health risk assessment of environmental radionuclides and heavy metals around a gold mining area in Gauteng Province, South Africa, Mahikeng: NWU.

Lapp, R. E. and Andrews, H. L., 1972. Nuclear Radiation Physics. London, Sir Isaac Pitman and Sons Ltd.

Lawson, R., 1999. Introduction to Radioactivity. Manchester.

Lilley, J., 2013. Nuclear physics: principles and applications. John Wiley & Sons.

Loden, L., 2011. Mining, milling, conversion and enrichment of uranium ores. [Online] Available at: https://www.youtube.com/watch?v=k7bkJ5nHF1c&t=2030s [Accessed June 2017].

Makhijani, A., Chalmers, L. and Smith, B., 2004. Uranium enrichment: Just plain facts to fuel an informed debate on nuclear proliferation and nuclear power. [Online] Available at: https://ieer.org/wp/wp-content/uploads/2004/10/enrichment.pdf [Accessed October 2017]

Masemola, B., Marumo, T.B., and Magampa, P.P., 2017. Enrichment measurements of UF4 unburnts material from a former uranium conversion plant in the republic of South Africa. Pretoria: NECSA.

Mashaba, M., 2011. Direct quantitative gross alpha beta - measurements of environmental water contaminated with nuclides from the uranium, thorium and actinium decay series and semi-qualitative indentification of nuclides concerned, Mafikeng: North-West University.

Mirion Technologies., 2011. MGAU. [Online] Available at: https://mirion.s3.amazonaws.com/cms4_mirion/files/pdf/specsheets/c39051_mgau_super_spec_1.pdf?1557863540 [Accessed 12 Septermber 2019].

Mirion Technologies., 2013. Model S573 ISOCS Calibration Software. [Online] Available at: https://mirion.s3.amazonaws.com/cms4_mirion/files/pdf/spec-sheets/c40166s573-isocs-calibration-software.pdf?1562764105 [Accessed 25 August 2019]

Morel, B. and Chatain, S., 2012. Comprehensive nuclear material: U–F system. Volume 2, pp. 199-204.

Nangu, M., Marumo, T., Mbedzi, E., and Rasweswe, M., 2014. ^{232}Thorium mass determination in a uranium/thorium mixture for safeguards purposes, Pretoria: NECSA.

National Nuclear Regulator, 2019. National Nuclear Regulator - History. [Online] Available at: www.nnr.co.za/history/ [Accessed 21 January 2019].

Necsa, 2018. Necsa - SAFARI- 1. [Online] Available at: www.necsa.co.za/services/safari1/ [Accessed 25 October 2018].

Nelson, D. and Reilly, G., 1991. Gamma ray interactions with matter: Passive non-destructive analysis of nuclear materials., Los Alamos National Laboratory.

Ng, K., 2003. Non-ionising radiations – sources, biological effects, emissions and exposures. Electromagnetic Fields and Our Health. Malaysia. pp. 1-16.

Onjefu, S., 2016. Natural radioactivity concentrations and occurrence of heavy metals in shore sediments along the coastline of the Erongo region in Western Namibia. Mahikeng: North West University.

Orrego, P., Hernandez, J., and Manriquez, J., 2016. Modeling operational parameters for uranium dioxide production reactor through uranium trioxide reaction using hydrogen. World Journal of Nuclear Science and Technology, Volume 6, pp. 131-139.

Parachoff, N., 1997. Marie Curie and the science of radioactivity. New York: Oxford University Press.

Parks, J.E., 2004. The Compton effect-Compton Scattering and gamma ray spectroscopy. University of Tennessee, Tennessee.

Prince, J. R., 1979. Comments on equilibrium, transient equilibrium, and secular equilibrium in serial radioactive decay. Journal of nuclear medicine: official publication, Society of Nuclear Medicine, Volume 20, pp. 162.

Raffo-Caiado, A., Begovich, J. M., Ferrada, J. J., Ladd-Lively, J., Marzo, M. A. S., Palhares, L. C., Diaz, F. C., and Grund, M.S., 2009. Model of a generic natural uranium conversion plant - suggested measures to stregnthen international safeguards. OAK RIDGE NATIONAL LABORATORY. Tennessee.

Ragheb, M., 2011. Gamma rays interactions with matter: nuclear, plasma and radiation science, s.l.: s.n.

Ridha, A.A., 2016. Nuclear Physics: Nuclear Detectors. 4th Grade Study guide. Baghdad, Al-Mustansiriya University.

Ruther, T. and Zsigrai, J., 2015. Recommendations for determining uranium isotopic composition by MGAU, Germany: s.n.

Shtangeeva, I., 2004. Thorium. Russia, St. Petersburg State University.

Sibbens, G., Moens, A. and Eykens, R., 2015. Preparation and sublimation of uranium tetrafluoride for production of thin $^{235}UF_4$ targets. Akademiai Kiado, Volume 305, pp. 723-724.

Silva M.D., 2015. Ionizing radiation detectors. Brazil. Intech Open.

Tohamy, M., El-Ghany, S. A., El-Minyawi, S.M., Fayez-Hassan, H., El-hakim E.H., El-Mongy S.A., and Comsan, M.N.H., 2016. Passive non-destructive assay based on gamma-ray spectrometry to verify UO_2 samples in the form of powder and pellet. Annals of Nuclear Energy, Volume 87, pp. 186–191.

Turner, J. E., 2007. Interaction of photons with matter. atoms, radiation, and radiation protection. Wiley-VCH Verlag GmbH & Co. KGaA.

UNODA., 2015. Review conference of the parties to the treaty on non-proliferation of nuclear weapons. [Online] Available at: https://www.un.org/en/conf/npt/2015/pdf/text%20of%20the%20treaty.pdf [Accessed 16 October 2019].

UNODA., 2019. Treaty on the non-proliferation of nuclear weapons. [Online] Available at: http://disarmament.un.org/treaties/t/npt [Accessed 14 October 2019].

DOE, 2001: Depleted uranium hexaflouride fact sheet: Characteristics of uranium and its compounds., U.S. Department of Energy Washington: s.n.

NRC, 1984. Non-destructive assay of special nuclear material contained in scrap and waste, United States Nuclear Regulatory Commision, Washington : s.n.

Venugopal, V., and Bhagdikar, P.S., 2013. de Broglie wavelength and frequency of scattered electrons in the compton effect. India. Physics Education.

von-Baeckmann, A., Dillon, G. and and Perricose, D., 1995. National reports: Nuclear verification in South Africa. [Online]

Available at: https://www.iaea.org/sites/default/files/publications/bulletin/bull37-1/37105394248.pdf [Accessed 10 September 2018].

von-Wielligh, N. and von-Wielligh-Steyn L., 2015. The bomb: South Africa's nuclear weapons programme. Pretoria. Litera Publication.

WNA., 2017a. The Nuclear Fuel Cycle. World Nuclear Association [Online] Available at: https://www.world-nuclear.org/information-library/nuclear-fuel-cycle/introduction/nuclear-fuel-cycle-overview.aspx [Accessed 15 October 2019]

WNA., 2017b. Conversion and deconversion. World Nuclear Association. [Online] Available at: https://www.world-nuclear.org/information-library/nuclear-fuel-cycle/conversion-enrichment-and-fabrication/conversion-and-deconversion.aspx [Accessed 13 June 2017].

WNA., 2017C. Thorium. World Nuclear Association. [Online] Available at: https://www.world-nuclear.org/information-library/current-and-future-generation/thorium.aspx [Accessed 13 June 2017].